

## 1. LEG 191 SUMMARY<sup>1</sup>

Shipboard Scientific Party<sup>2</sup>

### ABSTRACT

Ocean Drilling Program Leg 191 had two main goals: (1) to drill and case a borehole at a site in the northwest Pacific Ocean between Japan and Shatsky Rise and install therein a seismic observatory and (2) to test the drilling and casing emplacement capabilities of the hard-rock re-entry system (HRRS or "hammer drill") on a basaltic outcrop atop Shatsky Rise. There were also numerous ancillary scientific goals to be addressed using cores and logs obtained from Leg 191 sites. The seismic observatory was successfully installed at Site 1179 and left ready for activation by a future remotely operated vehicle cruise. The hammer drill tests were less successful owing to a streak of bad luck. Early in the leg, 4 days were lost when the *JOIDES Resolution* had to leave Site 1179 because of a typhoon. A medical emergency cost another 3 days and forced the ship to leave the Shatsky Rise area and return to Japan. In addition, a broken part on the drawworks made it impossible to return to Shatsky Rise for the HRRS tests. In an effort to salvage the HRRS program, the hammer drill was tested on a seamount near Guam (Sites 1180 and 1181), but the lithology was unsuitable (soft volcanic ash) and another typhoon forced evacuation of the area. Finally, an abbreviated HRRS test was accomplished at a site atop a basaltic volcano in the Mariana Trough (Site 1182).

Despite the operational difficulties, an excellent set of cores was obtained from Site 1179, which is located on lithosphere of Anomaly M8 age (129 Ma) (Gradstein et al., 1994, 1995). A 375-m-thick sedimentary column was cored in addition to 100 m of basaltic basement (total depth = 475 meters below seafloor). The sedimentary column can be divided into four lithostratigraphic units. Unit I consists of 221.5 m of clay- and radiolarian-bearing diatom ooze of late Miocene to late Pleistocene age. Ash beds are common in this unit, recording volcanic activity from the western Pacific island arcs. Unit II is a clay-rich, diatom-

<sup>1</sup>Examples of how to reference the whole or part of this volume.

<sup>2</sup>Shipboard Scientific Party addresses.

bearing radiolarian ooze of late Miocene age with a thickness of 24.5 m. Unit III contains barren brown pelagic clay in a 37.5-m-thick layer. Unit IV yielded poor recovery with only chert and porcellanite fragments from an unknown sedimentary host within 93.7 m above basement. The upper sedimentary section produced a well-defined magnetic reversal pattern, which shows that sedimentation was low (1.56 m/m.y.) before the mid-Miocene and increased 20-fold (to ~30 m/m.y.) in the Pliocene and Pleistocene. Biostratigraphy in Units I and II was based mainly on siliceous microfossils and palynomorphs, because calcareous microfossils were rare to absent. Sedimentation rates derived from biostratigraphy are in good agreement with those calculated from magnetostratigraphy. The brown pelagic clay of Unit III is barren, and few fossils were recovered from Unit IV; however, radiolarians observed in porcellanite samples indicate an Early Cretaceous age for the base of Unit IV. The physical properties of the upper sedimentary section are unusual because porosities are extremely high (often >80%) and bulk densities actually decrease downhole for the first 150 m. These characteristics probably result from an increase downward in abundance of diatom tests, which have low grain densities and contain large amounts of pore space. The 100-m igneous section consists of mainly aphyric ocean-ridge basalts divided into 48 units based on lithologic differences and cooling boundaries. The section consists of massive flows and pillows with small amounts of interunit sediments and volcanic breccia. The basalts are unusually fresh for Early Cretaceous igneous rock, and alteration is restricted to low-grade zeolite facies of temperatures less than ~10°–30°C.

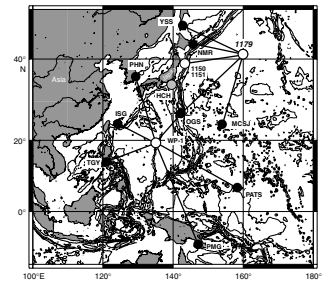
## INTRODUCTION

Tomographic studies using earthquake waves propagating through the Earth's interior have revolutionized our understanding of mantle structure and dynamics. A great limitation on existing tomographic images of the Earth's interior is the uneven distribution of seismic stations, especially the lack of stations in large expanses of ocean such as the Pacific. The International Ocean Network (ION) project, an international consortium of seismologists, has identified gaps in the global seismic observation network and is attempting to install digital seismometers in many of those locations. A high priority for ION has been to install a station beneath the deep seafloor of the northwest Pacific (Fig. F1) to gain a better understanding of regional earthquake patterns (Fig. F2) and to enhance tomographic images of the Earth's interior.

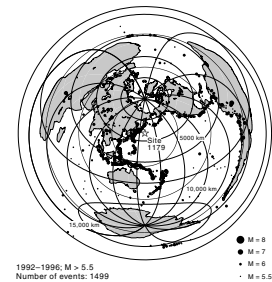
Installing a borehole seismometer at Site 1179 (proposed Site WP-2) in the northwest Pacific was one of two primary goals for Leg 191. That goal was accomplished at Site 1179, located on abyssal seafloor between Japan and Shatsky Rise (Fig. F3). The seismometer augments a regional network consisting of land stations in eastern Asia, Japan, and the western Pacific islands and borehole seismometers installed during Ocean Drilling Program (ODP) Leg 186 (Sacks, Suyehiro, Acton, et al., 2000) and planned for ODP Leg 195. Owing to its location, the Site 1179 seismometer will provide critical seismic observations from the seaward side of the Japan Trench (Figs. F1, F2).

Site 1179 is also important because it provides samples representative of the northwest Pacific Cretaceous oceanic crust and its sedimentary cover. Results from this site will augment those from Leg 185, which characterized material being subducted into the Mariana and Izu-Bonin

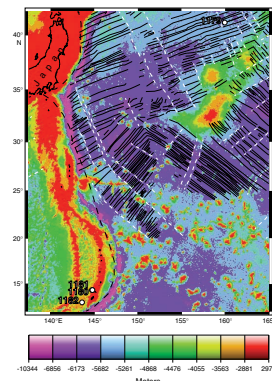
F1. Location map of seismic station coverage in the northwest Pacific, p. 22.



F2. Location of Site 1179 relative to circum-Pacific and other earthquakes, p. 23.



F3. Leg 191 site locations and magnetic lineations in the northwest Pacific, p. 24.



Trenches (Plank, Ludden, Escutia, et al., 2000), in addition to results from prior Deep Sea Drilling Project (DSDP) and ODP drilling in the region. Results from this site will also add to our knowledge of ocean crust structure, geochemistry, plate tectonics, magnetic lineations, sedimentation, and microbiology.

The second primary goal of Leg 191 was to test the hard-rock reentry system (HRRS), also known as the “hammer drill,” on a basaltic outcrop. The system uses a hydraulically actuated hammer that drives a drill bit into the ocean floor. Attached to the drill bit is a casing string that stabilizes the borehole walls and allows reentry into the hole with conventional ODP drilling and coring tools. The HRRS is important to long-term ODP science goals as a tool to be used for starting holes in difficult lithologies that would have previously prevented spudding the drill string. In particular, the HRRS is viewed as a tool that can start holes on bare, fractured igneous outcrops where drilling would otherwise be impossible. Testing of the HRRS was also undertaken during ODP Leg 179 but with limited success owing to delays caused by misdirected freight shipments, bad weather, and tool failure brought about by large heave during the test (Pettigrew, Casey, Miller, et al., 1999).

HRRS testing was planned for proposed Site SR-1, on a basaltic ridge atop the ocean plateau known as Shatsky Rise (Fig. F4). This site was chosen because it affords a bare basalt outcrop at a relatively shallow depth in a location convenient to Site 1179 and somewhat out of the main western Pacific typhoon track for late summer. Because of a medical emergency, bad weather, and problems with the ship’s drawworks, testing was moved from proposed Site SR-1 to an alternate location on a volcano a short distance from Guam.

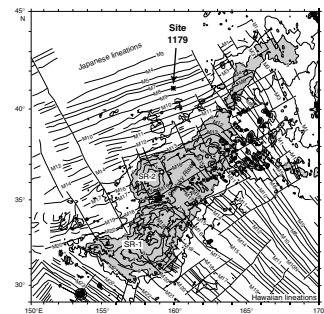
Despite difficulties encountered with delays forced by the weather, the medical emergency, and the broken drawworks, the seismometer was emplaced successfully, a good set of cores was recovered from Site 1179, and a partial HRRS test was accomplished. Consequently, Leg 191 goals were mostly met and the leg can be considered successful.

## **BACKGROUND**

### **Borehole Seismic Observatories**

The scientific importance of establishing long-term geophysical stations at deep ocean sites has been acknowledged by the Earth science and ODP communities and is detailed in various reports (JOI-ESF, 1987; Purdy and Dziewonski, 1988; JOI/USSAC, 1994; Montagner and Lancelot, 1995; ODP Long Range Plan, 1996). The objective is to understand the processes driving Earth’s dynamic systems from a regional to global scale by imaging the Earth’s interior with seismic waves. Unfortunately, few seismometers are located on the 71% of the Earth’s surface covered by oceans. The asymmetry and nonuniformity of seismic station distribution makes high-resolution imaging of some parts of the mantle nearly impossible. Ocean-bottom seismometers, whose locations have been carefully selected to optimize imaging (Fig. F1), are needed to accomplish the goals of international geoscience programs that use earthquake data. Aside from Site 1179, which was drilled and instrumented during Leg 191, several other western Pacific sites have also been selected for instrumentation. Observatories at Sites 1150 and 1151, located on the inner wall of the Japan Trench, were installed during Leg 186 (Sacks, Suyehiro, Acton, et al., 2000). In addition, proposed Site

**F4.** Site 1179 location relative to magnetic lineations in the north-west Pacific, p. 25.



WP-1, located in the Philippine Sea, is scheduled for drilling and instrumentation during Leg 195. Downhole instruments for these western Pacific borehole observatories have been developed under an ongoing national program within Japan (Ocean Hemisphere Project [OHP]). Data from these observatories will eventually become accessible worldwide through the OHP data center.

Aside from plugging an important gap in the global seismic array, the Site 1179 observatory will produce high-quality digital seismic data. Tests with other borehole seismometers show that the background noise level for oceanic borehole instruments is much less than most land counterparts (e.g., Stephen et al., 1999). Recent studies that exploit high-quality digital seismic data obtained on land have shown exciting new results pertaining to mantle flow. In the western Pacific, for example, Tanimoto (1988) showed that there exists a strong  $l = 2$  (angular order) pattern of deep (>550 km) high-velocity anomalies from waveform inversions of R2, G1, G2, X1, and X2 surface waves. This suggests a complex interaction of subducting slabs with the surrounding mantle, including the 670-km discontinuity, in the region (Tanimoto, 1988). However, because of sparse global coverage by existing seismic stations, current seismic wave resolution is insufficient to image the actual interaction of the plates with the mantle. More recent studies show the potential of new mantle imaging techniques, with finer scale images having been obtained in certain locations where high-quality data are dense. Two examples are the deep extension of the velocity anomaly beneath ridges (Zhang and Tanimoto, 1992; Su et al., 1992) and the fate of subducted plates at the 670-km discontinuity (van der Hilst et al., 1991; Fukao, 1992). These detailed results are possible because of the extraction of detailed information from existing seismograms. Such studies are limited by sparse data coverage, a barrier that new ocean-bottom stations can help break.

Scientific ocean drilling was introduced to ocean borehole seismometers during DSDP Leg 88 in 1982 when the *Glomar Challenger* drilled a cased hole at Site 581, ~320 km due north of Site 1179, and emplaced a seismometer built by the Hawaii Institute of Geophysics (Duennebie, Stephen, Gettrust, et al., 1987). The experiment confirmed that the deep-sea ocean crust is a quiet environment for seismic observatories (Duennebie et al., 1987), and it recorded a number of teleseismic events (Butler and Duennebie, 1987) including an earthquake of body-wave magnitude ( $M_b$ ) = 6.8 that occurred in Japan (Duennebie, 1987).

In September 1989, a feedback-type accelerometer capsule was installed in Hole 794D in the Japan Sea during Leg 128 (Ingle, Suyehiro, von Breyman, et al., 1990; Suyehiro et al., 1992, 1995). The instrument recorded a teleseismic event ( $M_b$  = 5.4 at an ~4000-km epicentral distance) that clearly showed a surface wave dispersion train (Kanazawa et al., 1992). In May 1992, a comparison of seafloor and borehole (Hole 396B) sensors was made using a deep-sea submersible for installation and recovery (Montagner et al., 1994). In 1998, another borehole seismometer was installed in Hole 843B, 225 km southwest of Oahu (Site 843) and has been used to improve understanding of the deep-sea seismic noise environment (Stephen et al., 1999). In August 1999 during Leg 186, digital broadband seismometers, strainmeters, and a tiltmeter were emplaced in boreholes at Sites 1150 and 1151 in the deep-sea terrace of the Japan Trench (Sacks, Suyehiro, Acton, et al., 2000). Data from these observatories have only recently been recovered by a remotely operated vehicle (ROV). Although at this stage there is no consensus as to how seafloor seismic observatories should be established, it

is becoming clearer that oceans can provide low-noise environments, especially when seismometers are placed into the igneous crust inside a borehole.

### **Tectonic Setting**

Leg 191, Site 1179 is located in the northwest Pacific Ocean east of Japan. The Mesozoic M-series magnetic lineations in the region (Fig. F4) show that the lithosphere in this area was formed in Late Jurassic to Early Cretaceous time (Larson and Chase, 1972; Sager et al., 1988; Nakanishi et al., 1989). Paleomagnetic studies indicate that this part of the Pacific plate formed  $\sim 30^\circ$  south of its present position, near or slightly north of the equator (Larson and Lowrie, 1975; Larson et al., 1992). The magnetic bight created by the intersection of “Japanese” and “Hawaiian” lineations implies that the spreading ridges that formed the lithosphere met at a triple junction that defined the northwest corner of the growing Pacific plate (Larson and Chase, 1972; Sager et al., 1988). Shatsky Rise, an oceanic plateau with an area about equal to Japan, began to form at the triple junction in latest Jurassic time coincident with a major reorganization of the spreading ridges and the triple junction (Sager et al., 1988; Nakanishi et al., 1989). Evidently the plateau formed rapidly at first, perhaps from a nascent mantle “plume head” (Sager and Han, 1993; Sager et al., 1999).

Sites 1180 and 1181 are located on an unnamed volcano located  $\sim 37$  km west of the island of Rota in the Marianas Island arc, whereas Site 1182 is situated atop a volcano formed at the southern end of the Mariana Trough backarc spreading center. These sites were chosen for HRRS testing as backup to the original primary and alternate sites because it became necessary to go to Guam to pick up spare parts for the ship’s drawworks. The Mariana arc is one of the major subduction zones of the western Pacific, where the Pacific plate converges with the trailing edge of the Philippine Sea plate (Karig, 1975; Hussong and Uyeda, 1982). Owing to divergence between the subducting Pacific plate and the retreating Philippine Sea plate, a series of several backarc basins have opened up between the two plates. The most recent of these is the Mariana Trough, which has formed since Miocene time and is located immediately westward of the Mariana arc (Karig, 1975). The volcano upon which Sites 1180 and 1181 are located is one that is known from bathymetric maps of the region near Guam and from a dredge taken from its northeastern flank for geochemical studies. The dredge recovered pumice boulders and basaltic andesite rocks (Dixon and Stern, 1983; Stern et al., 1989). Although the precise age of the volcano is not known, it appears to have erupted in recent geologic time but is not currently active. The spreading center volcano that is the location of Site 1182 is one that was known from dredge studies of the Mariana Trough. It also must be geologically young owing to its position on the active Mariana Trough spreading center.

### **Sedimentary Setting**

The history of the northwest Pacific plate since the formation of the lithosphere and Shatsky Rise is one of northward drift and low sedimentation. Sediments atop Shatsky Rise are as thick as 1.2 km because the rise top remained above the calcite compensation depth (CCD), allowing a thick layer of pelagic carbonate sediments to accumulate (Sliter and Brown, 1993). In contrast, sediments in the adjacent abyssal

basins are thin, typically 300–500 m thick (Ludwig and Houtz, 1979), owing to seafloor depth and distance from major sediment sources.

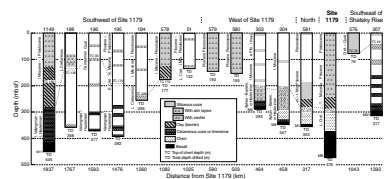
Cores collected in the northwest Pacific basin by DSDP (Legs 6, 20, 32, and 86) and ODP (Legs 185 and 191) over the last 30 yr show a similar stratigraphy with three primary layers (Fisher et al., 1971; Heezen, MacGregor, et al., 1973; Larson, Moberly, et al., 1975; Heath, Burckle, et al., 1985; Plank, Ludden, Escutia, et al., 2000). A Miocene to Pleistocene blanket of siliceous clay and oozes is present from the seafloor downward to >200 m in places. In these sediments, diatoms and radiolarians are common to abundant but few calcareous microfossils are found. Ash layers are also common. The Miocene to Pleistocene blanket of siliceous clay and oozes is largely absent or attenuated southeast of Shatsky Rise (Fig. F5). This observation implies that the thick Neogene layer results from higher productivity in waters of the mixing Oyashio and Kuroshio Extension currents. The gray to olive siliceous clays and oozes typically pass downward to barren brown or reddish brown clays. Although the age of these clays is often undetermined, at some sites they belong to the mid- to Late Cretaceous (e.g., Sites 51, 194, and 195) but this part of the column may contain a highly condensed Tertiary section as well (e.g., Site 576). Beneath the barren clays is an often poorly recovered layer consisting of calcareous oozes, chalk, or marl deposited soon after the formation of the crust while it was at a depth above the CCD. This layer has suffered poor recovery because it is associated with chert and porcellanite layers that are ubiquitous in the northwest Pacific. With rotary drilling using water as a flushing agent, the chert causes the formation to be ground up and the softer parts washed away, generally leaving only rounded chert fragments and slight traces of the softer matrix. In many holes, the top of the chert layer seems to correspond to the top of the calcareous section (Fig. F5) but this relationship is difficult to discern in some holes owing to poor recovery. In other holes, however, the chert appears higher in the section along with the barren brown clays.

## LEG OBJECTIVES

Leg 191 had two primary objectives. The first was to drill a cased re-entry hole into basement at proposed Site WP-2 (Site 1179) and install a broadband seismic observatory with a battery assembly and data-recording unit. The second was to perform engineering tests of the HRRS on a submarine igneous outcrop at a depth between 1000 and 2000 m. Leg 191 HRRS testing had three primary objectives: (1) characterization of the Model 260 fluid hammer operating parameters (i.e., flow rates, pump pressures, and weights on bit); (2) characterization of the hammer-drill and bit-spudding capabilities without casing; and (3) testing of the entire HRRS system by drilling in 20 m or more of 13.375-in casing in several slightly different fractured hard-rock environments. These hard-rock environments were to include (1) little or no overlying sediment or talus and little or no slope, (2) little or no overlying sediment but with a slope, and (3) a sloping surface covered with sediment or talus.

There were also numerous ancillary scientific goals that were envisioned related to cores or wireline logs obtained at the proposed drill sites. From Site 1179 drilling, we hoped to address the following areas: structure, geochemistry, and isotopic characteristics of the upper ocean crust, Pacific plate paleolatitude and tectonic drift, the age of magnetic

**F5.** Comparison of stratigraphic columns at Site 1179 and other boreholes in the northwest Pacific, p. 26.



Anomaly M8, and the microbiology of the abyssal sediment column. It was also hoped that cores would be recovered from Shatsky Rise during the course of the engineering test and that those cores would yield important data about the age and geochemistry of that large igneous province.

The sediment column and igneous basement at Site 1179 were cored successfully, and the borehole seismometer was emplaced as planned. Consequently, it should be possible to accomplish the scientific objectives related to coring and placement of the seismic observatory. The logging program, however, was seriously curtailed owing to collapse of the borehole that did not allow either the lower part of the borehole to be logged or most logs to be run. In addition, because of a streak of bad luck that included a medical emergency and a broken part on the drawworks, it was necessary to move the HRRS tests to a site close to Guam. As a result, the Shatsky Rise objectives were not addressed and the HRRS tests were shortened. However, the abbreviated tests went well and the HRRS tests goals related to hammer operation and spudding characteristics were successfully completed (Tables T1, T2).

## SYSTEMS OVERVIEW

### WP-2 Borehole Seismic Observatory

The WP-2 broadband seismic observatory (Fig. F6) is designed to last for many years deep beneath the sea. Because there are no coaxial transoceanic telephone cables near Site 1179 to utilize for data recovery and power, the WP-2 installation was designed as a stand-alone system with its own batteries and data recorder. Two seismometers have been installed in Hole 1179E, each housed in a separate pressure vessel. Both sensors are feedback-type broadband seismometers (Guralp Systems Ltd., CMG-1T). The borehole seismometers were cemented into the hole to make good coupling to the host rock and to avoid noise caused by water circulation near the seismometers. Two separate cables are connected to the sensors and carry signals and power between these instruments and other system modules at the seafloor. The signals are digitized in the sensor packages and sent in digital form to a data-recording unit in the seafloor electronics package.

The seafloor package, called the MEG-191, combines the digital data from the two seismometers into a single serial data stream and distributes power to the individual seismometers. The data are stored in digital format in a separate module, called the SAM-191, transmitted via an RS232C link. The SAM-191 has four 18-GB SCSI hard disks, which allow more than 1.5 yr of continuous data recording with 24-bit dynamic range at a 100-Hz sampling rate from the two seismometers. The MEG-191 can be physically replaced by an ROV or submersible and accepts commands and software upgrades through the SAM-191. The SAM-191 is designed for servicing by an ROV or submersible. Before the disks become full, it can be swapped for an “empty” unit. Additionally, the ROV or submersible can download part of the data stream via a serial link, so operators can check the health of the borehole system. The SAM-191 also measures the time difference between the clocks in the SAM-191 and the MEG-191. Before deployment and after retrieval of the SAM-191, the time difference between the clock within the SAM-191 and the Global Positioning System (GPS) clock is measured so time-based corrections can be applied.

---

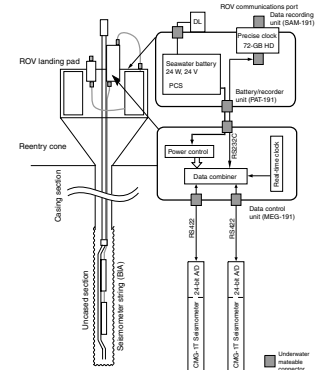
T1. Coring summary, p. 48.

---

T2. Extended coring summary, p. 49.

---

F6. Schematic of the WP-2 seismic borehole observatory, p. 27.



All station power is supplied from the seawater battery (SWB) system. The SWB can supply up to ~24 W with a >400 kWh capacity. Its energy comes from electrolytic dissolution of the magnesium anode. The condition of the SWB system is continually monitored by the power control system (PCS), and data from the PCS are recorded in the data logger (DL). In addition, the PCS controls the power switch and shuts off the observatory, for the protection of the system, if the SWB provides either too much or too little power.

### **Hard-Rock Reentry System**

The HRRS is being developed to provide ODP with the ability to spud and to establish a reentry casing on sloped and fractured hard-rock outcrops on the seafloor. The system uses a Model 260 downhole fluid hammer developed by SDS Digger Tools of Canning Vale, Western Australia, along with a bit to advance the hole while casing, installed simultaneously. At present, 13.375-in casing is being used in the prototype development program. The rough seas encountered during Leg 179 tests demonstrated the need for more robust bits that could withstand the torque, lateral pivoting (i.e., rocking) movements, and weight-on-bit fluctuations experienced during this first offshore trial. All three of these parameters contributed to the premature failure of the bits tested during that leg (Pettigrew, Casey, Miller, et al., 1999).

The next generation of bits developed for the Leg 191 HRRS testing program was tested on shore. Corrections and improvements to the bits were made based on the observations of these land tests. Despite the limited onshore testing, the next generation of bits appears much superior to those used during Leg 179.

Two new bit types were developed for testing during Leg 191; these include underreamer and ring-type bits. Two different versions of the underreamer bits were tested as well as two versions of ring-type bits. Underreamer bits have retractable arms to open a larger hole than the pilot bit onto which they are mated. Ring bits are composed of two major parts that include a casing shoe and pilot bit. The casing shoe has a ring of tungsten carbide buttons that works in tandem with the pilot bit. However, unlike the underreamer bits, which are totally recovered at the completion of the installation process, the casing shoe is left in the hole on the bottom of the casing after the pilot bit and hammer are withdrawn.

## **OPERATIONS**

### **Coring in Holes 1179A to 1179D**

The transit from Yokosuka, Japan, to Site 1179 began at 0800 hr on 22 July 2000 (Universal Time Coordinated [UTC] + 9 hr) and was completed on 25 July at an average speed of 12.5 kt. At 1545 hr on 26 July, the initial advanced piston coring (APC) core recovered 10.0 m of siliceous ooze but the full core did not accurately establish the mudline. To provide extra material for sampling near the seafloor, this core was curated as the first and only core of Hole 1179A. Hole 1179B was spudded at 1700 hr on 26 July. This time a 7.6-m mudline core was recovered, establishing a seafloor depth of 5563.9 meters below sea level (mbsl). APC coring proceeded through Core 191-1179B-6H to a depth of 55.1 meters below seafloor (mbsf). The Lamont Doherty Earth Observatory (LDEO)

drill string accelerometer (DSA) tool was deployed on top of the Core 191-1179B-7H core barrel, and a rubber centering ring on the tool caused the core barrel to become stuck in the drill string at a depth of about 650 meters below rig floor (mbrf). Recovering the stuck core barrel required lifting the drill string clear of the seafloor, ending Hole 1179B at 0400 hr on 27 July.

Hole 1179C was spudded at 1400 hr on 27 July 2000. Recovery from the first core established a seafloor depth of 5563.9 mbsl. The hole was washed to a depth of 48.8 mbsf, where continuous APC coring was resumed at 6.3 m above the total depth (TD) of Hole 1179B. APC coring continued to a depth of 266.8 mbsf (Core 191-1179C-24H), where an incomplete stroke necessitated the end of piston coring. The DSA tool was deployed successfully on Cores 191-1179C-4H and 7H without the rubber centering ring installed. Of the 223.8-m cored interval, the APC recovered 230.42 m of core (103.0% recovery). Extended core barrel (XCB) coring began with Core 191-1179C-25X and continued through Core 27X to a depth of 292.9 mbsf, where chert stringers caused the destruction of a hard formation shoe. The APC/XCB drilling assembly was pulled clear of the mudline at 1310 hr on 29 July. Hole 1179C was cored to a TD of 292.9 mbsf. The maximum drill string deployed was 5869.6 mbrf. A total of 246.89 m of core was recovered for an overall average recovery of 98.8%. Of the 26.1 m penetrated with the XCB, 16.47 m, or 63.1%, of core was recovered.

Tensor tool orientation data were taken for Cores 191-1179B-4H through 6H and for Cores 191-1179C-3H through 11H and 13H-24H. Adara temperature measurements were taken from Cores 191-1179C-3H (67.8 mbsf; 5.5°C), 6H (96.3 mbsf; 7.7°C), 9H (124.8 mbsf; 8.2°–8.8°C), and 12H (153.3 mbsf; 11.2°–11.7°C). Perfluorocarbon tracer (PFT) was pumped into the drilling fluid for microbiological studies of drilling fluid contamination during deployment of Core 191-1179B-5H and Cores 191-1179C-21H and 27X.

Hole 1179D was spudded at 0300 hr on 31 July. Drilling continued with a rotary core barrel (RCB) center bit in place to a depth of 281 mbsf. An RCB core barrel was then pumped to the bottom to initiate coring approximately one core above the TD of Hole 1179C. Coring was difficult in this interval because of chert layers. A total of nine cores were recovered through the chert zone. Of the 86.5 m penetrated, <6 m of core was recovered (6.7% recovery). The basement contact was cored in Core 191-1179D-10R at an estimated depth of 375 mbsf. Coring continued 100 m into basaltic basement through Core 191-1179D-22R to a TD of 475 mbsf. Of the 100 m of basalt cored, 43.5% was recovered.

Once coring was suspended, the hole was prepared for logging first by circulating and making a wiper trip up to 150 mbsf and back to TD. The bit was released and the end of the drill string was positioned at ~150 mbsf (slightly deeper than normal because of the exceptionally soft sediments in the upper sediment column). The triple-combination (triple combo) tool string (phasor dual-induction tool [DIT], high-temperature lithodensity tool [HLDT], acceleration porosity sonde [APS], and hostile-environment natural gamma sonde) with the LDEO temperature/acceleration/pressure tool and a high-resolution multisensor gamma-ray tool (MGT) was run in the hole, making this the longest wireline tool string (>130 ft) ever deployed by ODP. The logging run consisted of two planned passes plus some short repeat runs for data quality verification. A first pass in the logged depth interval was required for recording Schlumberger triple-combo data and the second for running the LDEO MGT. The tool string was lowered to 300 mbsf,

and the run was reversed, moving up ~100 m. When the tool was once again lowered, it was not able to pass ~260 mbsf. After repeated efforts to pass this depth were unsuccessful, the remaining hole was logged up to the mudline. After logging concluded, the drill string was lowered to a depth of 377 mbsf and a cement plug was set to ensure that there would be no communication of seawater downhole and through fractures to the instrument installation in Hole 1179E. The end of the drill string reached the rig floor at 1150 hr on 6 August, ending Hole 1179D.

### **Drilling Operations for Borehole Instrumentation Deployment: Hole 1179E**

At 1145 hr on 6 August, Hole 1179E was spudded using a bottom-hole assembly (BHA) with a reentry cone and a 16-in casing hanger assembly at a seafloor depth of 5566.0 mbsl. Within 2 hr, the casing was jettied in and the Dril-Quip (DQ) running tool was released from the reentry cone/casing assembly. The drill string was assembled with a tri-cone bit, and at 0715 hr, Hole 1179E was reentered and the drill pipe was run in the hole to just above the 16-in casing shoe located at ~64 mbsf. Drilling of Hole 1179E was initiated and basement was ultimately contacted at ~371.0 mbsf. Drilling continued into the basement to a depth of 399.0 mbsf (~28.0 m into basement). The drill string was recovered, and preparations began for making up and deploying the 10.75-in casing string. At 0230 hr, Hole 1179E was reentered for the second time and the 10.75-in casing string was run to bottom without incident. The casing hanger landed out with the shoe placed at a depth of 393.4 mbsf. A cement slurry was pumped into the hole to firmly attach the casing into the host rock. The DQ running tool was released within an hour, and at 0900 hr, the cementing swivel and top drive were laid out and the pipe trip out of the hole was begun. All tools were clear of the rotary table by 0300 hr on 14 August; however, further drilling operations were halted because a tropical storm was headed toward the drilling location.

By 0800 on 14 August, all of the drill collars had been safely stored in the racks and the ship was secured for transit in possible heavy weather. The ship then entered a waiting-on-weather mode. When the tropical storm intensified into Typhoon Ewinia, it was necessary to abandon the site. Eventually, the storm weakened and Site 1179 was reoccupied. With the storm downgraded to a tropical depression and no longer a threat to drilling at Site 1179, the thrusters were dropped at 0930 hr on 18 August and work on site was resumed. Including the time to lay out and pick up the 8.25-in drill collars, the avoidance of Typhoon Ewinia cost a total of 104 hr (4.3 days) of operating time. A total of 909 nmi was transited during this period at an average speed of 10.1 kt.

The drilling assembly was made up and run in the hole. Hole 1179E was reentered for the third time at 2230 hr on 18 August. Reentry time was 45 min. The bit was advanced, and by 0615 hr on 19 August, basement drilling began. Drilling proceeded until a TD of 475.0 mbsf was achieved at 0115 on 21 August. Drilling was consistent throughout the basement interval, averaging 2.0 m/hr. Based on drilling data, the hole appeared to be in excellent condition for installation of the two CMG-1T broadband seismometers. The bit reached the rotary table at 1445 hr on 21 August 2000, ending the reentry cone, casing, and drilling preparations for Hole 1179E.

## Installation of the Seismic Observatory

The primary objective of Site 1179 was to establish a seismic borehole observatory in the upper igneous crust on abyssal Pacific lithosphere in order to record high-quality seismic data for monitoring earthquake waves from around the globe. The plan was to install two Guralp CMG-1T three-component broadband seismometers within the upper 100 m of igneous basement because studies have shown that igneous basement is an especially quiet environment at seismic frequencies. After studying the igneous section drilled in Hole 1179D, it was decided to place the seismometers at a depth of about 90 m (461 mbsf) into the igneous rock. From measurements of physical properties, average densities and velocities in the basalt section were 2.754 g/cm<sup>3</sup> and 5002 m/s, respectively.

At 1445 hr on 21 August, we began to install the seismic borehole observatory in Hole 1179E. The borehole instrument assembly (BIA) was made up to a joint of 4.50-in casing, and the stinger pipe and the BIA were then lowered down to the moonpool level using the 4.50-in casing elevators. The two instrument cables were fed from their respective reels over sheaves hung below the rotary table and connected to the CMG-1T seismometers. After testing the seismometers through the instrument cables, the 4.50-in casing and cable deployment operation began in earnest at 1830 hr on 21 August. Each joint of 4.50-in casing was run with two electrical cables strapped to the outside and secured with tie wraps and duct tape. Approximately every 1.5 m, a 4.50-in casing centralizer (measuring ~9 in outer diameter) was attached. Nineteen joints (221.3 m) of casing were run at ~5 joints/hr, and then a circulating sub (0.34 m) was installed. Another 19 joints (221.8 m) of casing followed before it was time to pick up the riser/hanger assembly. The riser/hanger was connected to the J-slot running tool and the last joint (11.65 m) of 4.50-in casing. The assembly was lowered through the rotary table, and the slips were set on a 10-ft drill collar pup joint attached to the J-tool. The instrument cable was cut to length, and the long and tedious cable terminating process began at 0500 hr on 22 August in the subsea shop. It was completed, along with associated electrical tests, later that same day at 2200 hr.

With the cable terminating process completed, the cables were then strapped onto the last two joints of 4.50-in casing and the MEG-191 was installed into the multi-access expandable gateway (MEG) frame on the riser/hanger (Fig. F7). By 0130 hr on 23 August, the instrument string assembly and final electrical integrity checks were completed. The remainder of the BHA was assembled, the drill string was lowered, and Hole 1179E was reentered for the fourth and final time at 1115 hr on 23 August. The instrument package was lowered into the hole without incident, and at 1500 hr on the same day, the riser/hanger landed at the right depth. A 50-bbl slurry of cement was mixed and pumped downhole, cementing the instruments in place with the end of the stinger located at a depth of 467.2 mbsf (96.2 m into basaltic basement). Using theoretical hole volumes and displacements, the top of the cement slurry should have reached a level of ~112 m above the 10.75-in casing shoe.

Once the drill string was adequately flushed, the vibration-isolated television (VIT)/subsea television (TV) system was recovered. Preparations then began for deploying the power access terminal (PAT; the frame for the seawater batteries) and continued through 0215 hr on 24 August. These included tack-welding the frame structure and rigging

F7. MEG-191 system controller attached to the riser/hanger assembly prior to installation, p. 28.



the deployment bridle and the three glass balls for cable retraction, redundant acoustic release package, and the wire cables for transferring the weight of the platform to the logging line. After standing by for 1.25 hr, waiting for enough daylight to see below the water line in the moonpool, the final rig-up of the logging line was completed and the PAT was lowered through the moonpool at 0415 hr 24 August (Fig. F8). The 4.75-hr trip ended at 0900 hr, when the PAT landed in the reentry cone. The PAT was released from the bridle by an acoustic command. After rigging down the platform deployment bridle assembly, the VIT/subsea TV system was deployed to survey the platform installation and observe the J-tool release from the riser/hanger (Fig. F9). By 1445 hr on 24 August, the camera was down, proper platform installation was verified, and the J-tool was released. The installation of the seismic borehole observatory in Hole 1179E was complete (Fig. F10).

**Transit to Site 1180**

At ~0800 hr on 25 August, with the nondestructive testing of the drill collars still in progress, it was necessary to halt operations because of a medical emergency that required evacuating a crew member to Japan. The remainder of the BHA inspection was canceled. The remaining drill collars were laid out and the rig was secured for transit as quickly as possible. At 0845 hr on 25 August, the *Resolution* got under way at full speed for Kushiro, Japan, a port city on the island of Hokkaido.

At 1345 hr on 26 August, a helicopter from the Japanese Coast Guard ship *Soya* landed on the helideck to take the doctor and patient the rest of the way to Japan. Because the *Resolution* could not resume work until the doctor returned, the ship continued to steam toward Kushiro. At 0720 hr on 28 August, a transport helicopter returned the doctor to the ship. In the meantime, a routine inspection of the brake bands on the drawworks winch found a crack that could not be repaired because there was no spare on board. Consequently, hammer drilling at Shatsky Rise was cancelled. Instead, the ship turned toward Guam, the final destination of Leg 191, in hopes that spare parts could be flown to Guam ahead of the ship. The next 7 days were spent in transit.

During the transit, the co-chiefs and staff scientist began trying to find a site suitable for HRRS testing near Guam with the idea of getting the new brake band, installing it at sea, and setting up an abbreviated HRRS test. A site with an igneous outcrop was desired, with a water depth between 1000 and 2000 m. A colleague on shore suggested a volcano in the Mariana arc located about 37 km west of the island of Rota, less than a half-day cruise from Guam. Clearances to drill were rapidly obtained.

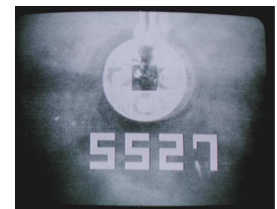
**Sites 1180–1181: HRRS Tests**

After obtaining replacement parts in a rendezvous off Rota Island with the supply boat *Shamrock* at 1415 hr (UTC + 10 hr) on 3 September, repairs were quickly made and the drawworks put back in order. A short survey was conducted of the target seamount using the 3.5- and 12.0-kHz echo sounders and magnetometer. The echo sounders showed that the slopes of the seamount were relatively steep for the HRRS test, typically about 14° on most flanks. A spot on the middle flank at a depth of about 2160 m was chosen because the slope angle seemed slightly less at this location. The VIT/subsea TV camera was run to examine the seafloor. The ocean floor appeared firm but sedimented de-

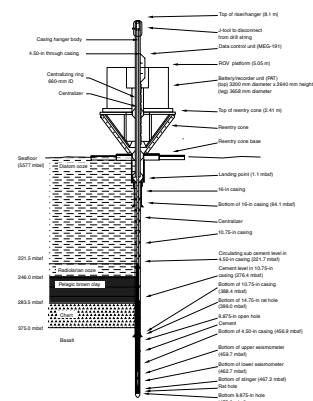
**F8.** Power access terminal battery frame being lowered through the moonpool, p. 29.



**F9.** Snapshot showing the PAT landed properly on top of the Hole 1179E reentry cone, p. 30.



**F10.** Schematic of the borehole seismic observatory installation in Hole 1179E, p. 31.



spite the steep slopes. Because there was no evidence of a sediment veneer on the 3.5-kHz echo-sounder profiles, it was decided that drilling should be attempted. A BHA with the hammer drill was rigged, tested, and sent to the seafloor. At 1315 hr on 4 September, Hole 1180A was spudded at 14°18.52'N, 144°44.75'E. The drill string quickly sank into the soft, sandy sediments, which are interpreted as volcanic ash. The hammer was unable to come to full pressure because fluid circulation flushed the sediments away, allowing the BHA to jet in. After 30 min and 5 m of penetration, the collapsing hole walls dictated pulling the BHA free. Twice more the hammer was tried at different locations with the same results. The greatest penetration at Site 1180 was 8 m.

The drill string was raised and the ship moved 3 nmi upslope to the rim of a large crater on the west side of the seamount at a depth of ~956 m. The hammer was rigged again and run to the bottom. Hole 1181A commenced at 0115 on 5 September in what appeared on the VIT/subsea TV camera to be coarse rubble (14°19.26'N, 144°48.00'E). As at Site 1180, the drill quickly penetrated the bottom by flushing away the volcanic ash and debris until circulation was lost and the hole collapsed on the BHA. Three holes were tried at Site 1181, all with similar results. The maximum penetration of the drill string at Site 1181 was 3 m. After surveying the seafloor with the VIT/subsea TV camera across the top of the crater rim and into the crater, we decided that this flank of the seamount was primarily composed of nonindurated ash and debris. The drill string was tripped to the rig floor, and preparations were made to survey the other side of the seamount.

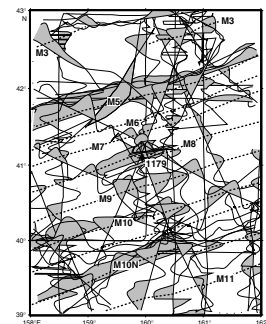
Before the pipe trip was finished, weather reports indicated that a tropical low located east of Guam was intensifying and would turn into a typhoon (named Saomai) and Rota was in its path. The *Resolution* quit the site and headed southwest ahead of the storm. In disgust, the name *Inutil*, which is Spanish for “worthless,” was bestowed on the unnamed seamount.

After a short transit past Guam, the *Resolution* conducted a brief survey over a seamount on the backarc spreading center of the Mariana Trough. The seamount was found to have a relatively flat summit at a depth of ~2880 m, which seemed suitable for drilling. The hammer was rigged and sent to the bottom with the VIT/subsea TV system. The camera showed the rough pillowed surface of a submarine lava flow. Hole 1182A was spudded at 0845 hr on 5 September, at 12°57.00'N, 143°36.66'E. For the next 57 hr, spud tests with both types of drill bits and the vibration-damper sub were conducted successfully at Holes 1182A–1182F. By 1800 hr on 7 September, spud tests were finished but insufficient time remained for making up a casing assembly and testing that part of the HRRS system. Consequently, the drill string was tripped back to the rig for the last time, clearing the rotary table at 0800 hr on 8 September. Having accomplished its missions for Leg 191, the *Resolution* sailed to Guam, arriving at 1400 hr on 8 September.

## SITE 1179 SCIENTIFIC RESULTS

Site 1179 is located at 41°04.8'N, 159°57.8'E, on abyssal seafloor north of Shatsky Rise. The site is situated on an east-northeast–trending magnetic lineation interpreted as M8 (Figs. F4, F11), making the lithosphere at this site ~129 Ma in age (mid-Hauterivian stage) according to the Gradstein et al. (1994, 1995) time scale.

F11. Magnetic lineations in the vicinity of Site 1179, p. 32.



## Sedimentary Lithology

Four sedimentary units with a total thickness of 375 m overlie basaltic crust at Site 1179 (Figs. F12, F13). From the seafloor downward they range in age from the present to an as-yet-undetermined time in the Early Cretaceous. Unit I, at the top of the section, consists of clay- and radiolarian-bearing diatom ooze (Fig. F14). It extends from the seafloor to a depth of 221.5 m, where it is late Miocene in age. The siliceous oozes of Units I and II have three principal components: diatoms, radiolarians, and clay, with proportions that vary from core to core. Diatoms predominate in Unit I, radiolarians are common, and sponge spicules and silicoflagellates contribute to the siliceous nature of the sediment. A range of greenish colors and intervals of ichnofossils and laminations suggest that the diatom ooze was deposited in a dysoxic bottom environment; neither anoxic nor fully oxic conditions prevailed for any extended length of time. Sediment accumulated faster in Unit I than in the other units, a factor that may have contributed to the dysoxic environment. The diatom ooze resembles other Neogene sections cored in the northwest Pacific (Fig. F5), with its beds of gray silicic vitric ash of a few centimeters thickness, numerous thin, firm dark green clay layers, and contributions of illitic clay, quartz, and glass within the ooze.

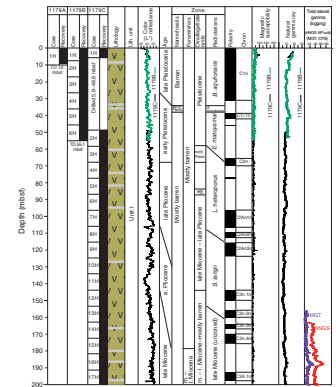
The contact between Units I and II is gradational, both in color and composition, as olive-colored diatomaceous ooze gives way to yellowish brown radiolarian ooze. The top of Unit II is placed at the base of Chron C4n.1n, below which radiolarians predominate. This clay-rich diatom-bearing radiolarian ooze is 24.5 m thick. It extends to 246.0 mbsf, where it is of early late Miocene age. Accumulation was slower than in Unit I. The brown coloration, mottling by burrowing, and a virtual lack of other sedimentary structures indicate an oxic environment (Fig. F15). The base of Unit II is also a gradational one, where radiolarian remains vanish downward and the clay of Unit III prevails. In time, this contact represents the return of the deposition and preservation of siliceous microfossils in the North Pacific during the Miocene.

The pelagic brown clay of Unit III is ~37.5 m thick and extends down to ~283.5 mbsf. Its age is unknown, as it is barren of fossils except for a few fish teeth and bone fragments, and there is no clear pattern of magnetic reversals except in the upper ~11 m. The clay is zeolitic, ferruginous, mottled, and compact (Fig. F16). Core recovery was excellent (101.4%) in all of Units I, II, and III. Unit IV is chert residing in an unknown host formation that was not recovered. It extends from 283.5 to 377.15 mbsf, and its age has yet to be determined. Recovery of this 93.65-m-thick section was poor (6.7%), both as a percentage of the penetration and in the degree of fracturing. Most pieces are of vitreous chert (Fig. F17), with a wide range of colors, mottling, healed brecciation, and veins, but a few are pieces of porcellanite. A fauna of poorly preserved radiolarians in the porcellanite appear to be Early Cretaceous in age and may allow better shore-based determination of age of at least part of the cherty section.

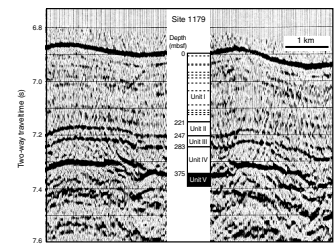
## Igneous Petrology

Core 191-1179D-10R recovered chert and basalt at a depth of 375 mbsf. The actual contact between the two lithologies was not recovered. Coring of basalt continued to a TD of 475 mbsf, ending with Core 191-1179D-22R. Basement rocks recovered in Hole 1179D consist

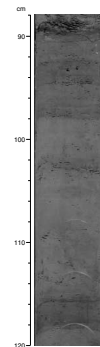
F12. Lithostratigraphic summary column for Site 1179, p. 33.



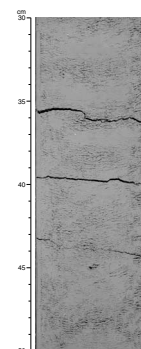
F13. Comparison of the site survey, the lithostratigraphic column at Site 1179, and lithostratigraphic boundary depths, p. 37.



F14. Clay- and radiolarian-bearing diatom ooze of Unit I, p. 38.



F15. Clay-rich diatom-bearing radiolarian ooze of Unit II, p. 39.



mostly of fresh aphyric basalts in massive flows (Fig. F18), pillows, and breccia, with a minor amount of interpillow sediments. The section is divided into 48 igneous units based on lithologic differences and flow and/or cooling unit boundaries (Fig. F19). Based on mineral presence and abundance in hand samples and thin sections, three groups of basalts were categorized: olivine-poor basalt (Group I), olivine-free basalt (Group II), and olivine-rich basalt (Group III). The basalt of the upper eight units belongs to Group I. The basalt of the middle 16 units belongs to Group II. All of the basalt from the lower 24 units belongs to Group III. The most distinct petrologic change among the cored basalt occurs between Units 24 and 25, where the difference in content of altered olivine grains causes a distinct color change.

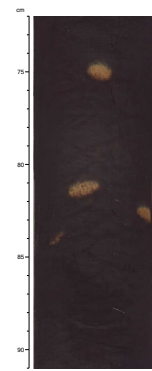
Olivine-poor and olivine-free basalts are fine grained with subophitic texture, whereas the olivine-rich basalts have medium grain sizes with ophitic fabric in the thicker massive lava flows. Glass rims from chilled margins on pillows and massive lava flows are mostly palagonitized; near-border parts are now hyalopilitic or cryptocrystalline to microcrystalline. The groundmass of the basalts consists dominantly of lathlike plagioclases and clinopyroxenes (Ti-augites) and almost completely recrystallized glass/palagonite as mesostasis. Very fine grained magnetite is concentrated in the altered glass; Cr spinel, apatite, and very rare zircon are accessories. Olivine in the matrix of Group III basalts is almost completely changed to iddingsite, as are the olivine phenocrysts in Groups I and III. Plagioclase phenocrysts are mostly fresh but partly corroded or replaced. The primary mineralogy of the basalt from Site 1179 is consistent with mid-ocean-ridge basalt rather than ocean-island (alkali) basalt. Secondary mineralogy embraces calcite, celadonite, saponite, smectite, and zeolites, filling fissures, veins, and vesicles. Alteration of the basalt is surprisingly low and belongs to the low-grade zeolite facies in a possible temperature range of 10°–30°C.

### Biostratigraphy

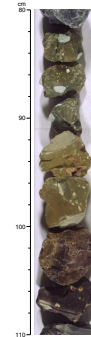
Because Site 1179 has been beneath the CCD for tens of millions of years, biostratigraphy for this site relies mainly on the identification of siliceous microfossils and palynomorphs. Siliceous microfossils (radiolarians, diatoms, and silicoflagellates) are common and generally well preserved in lithostratigraphic Units I and II at Site 1179. They were absent from the red pelagic clays of lithostratigraphic Unit III and generally poorly preserved (recrystallized) in the cherts of lithostratigraphic Unit IV. Numerous radiolarian datums were identified, and upper Miocene to upper Pleistocene sediments can be assigned to established radiolarian zones, providing good biostratigraphic resolution. Two radiolarian species are identifiable in a single chert sample near the basaltic basement, indicating an Early Cretaceous age for the oldest sediments at this site.

Terrestrial spores and pollen and marine dinocysts and acritarchs are present and moderately to well preserved in all samples examined in the upper ~144 m of lithostratigraphic Unit I. All of these samples are of late Pliocene to late Pleistocene age, except for the lowermost palynomorph-bearing sample examined (Sample 191-1179C-11H-CC; 143.84 mbsf), which is of late early Pliocene age. All other sediments in lithostratigraphic Unit I and all of lithostratigraphic Units II, III, and IV are barren of palynomorphs. A number of dinocyst datums can be identified, providing good stratigraphic resolution in sediments of late Pliocene to Pleistocene age. Terrestrial palynomorphs (pollen and

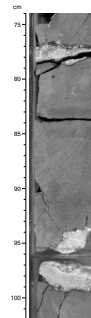
**F16.** Brown pelagic clay found in Unit III, p. 40.



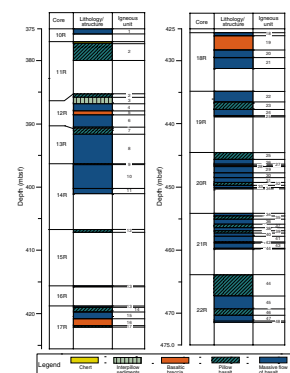
**F17.** Chert fragments recovered from Unit IV, p. 41.



**F18.** Basalt from Unit V, p. 42.



**F19.** Summary of igneous units in the basaltic basement section, p. 43.



spores) are most abundant in sediments of Pleistocene age and in those upper Pliocene sediments with anomalously high CaCO<sub>3</sub> content, where they sometimes outnumber dinocysts.

The only core-catcher sample that contains calcareous microfossils (calcareous nannofossils and planktonic and benthic foraminifers) is Sample 191-1179B-4H-CC (36.02 mbsf). The foraminifers are not biostratigraphically useful, but calcareous nannofossils indicate an early Quaternary age for this sample. There is no explanation at this time for the preservation of calcareous microfossils in this sample and in several other samples within cores of late Pliocene to early Pleistocene age in which routine inorganic geochemical analysis and palynological processing identified anomalously high carbonate content.

Agglutinated foraminifers are present in some upper Miocene to upper Pliocene samples, and the presence of the finely agglutinated taxon *Spirosigmoinella compressa* constrains the 229.77- to 181.94-mbsf interval to middle to late Miocene. No calcareous nannofossils or foraminifers are found in lithostratigraphic Units III or IV.

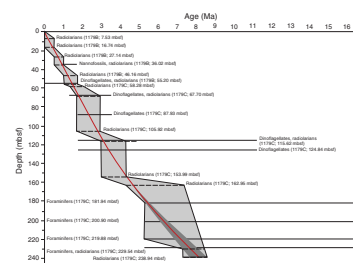
Sediment ages derived from biostratigraphic datums (radiolarians, dinoflagellate cysts, benthic foraminifers, and calcareous nannofossils) in the upper Miocene to upper Pleistocene sequence at Site 1179 are plotted against depth in Figure F20. Biostratigraphic resolution is highest in Pleistocene sediments and lowest in the upper Miocene–lower Pliocene sediments. The shaded area encompasses the minimum and maximum ages for each sample, constraining sediment accumulation rates. Sedimentation rates were high and relatively constant throughout the late Cenozoic, averaging ~35 m/m.y. during the Pliocene–Pleistocene and ~30 m/m.y. during the late Miocene.

### Paleomagnetism

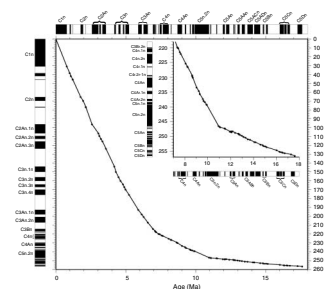
The sediments of Units I and II contain an excellent magnetostratigraphic sequence. In the six cores of Hole 1179B, the Brunhes (C1n) and Matuyama (C1r) magnetic chrons and the Jaramillo (C1r.1n) and Cobb Mountain (C1r.2r1n) magnetic subchrons are found. The sedimentation rate for the Brunhes Chron, based on 31 m over 0.78 m.y., is 39.7 m/m.y. (Fig. F21). The first core of Hole 1179C contains the mudline and is in the Brunhes Chron. The hole was deepened to the approximate end of Hole 1179B before coring resumed. Cores 191-1179C-2H through 18H record the Matuyama (C1r), Olduvai (C2n), Reunion (C2r.1n), Gauss (C2An), Gilbert (C2Ar, C3n, C3r), and C3An magnetic chrons. The sedimentation rate between the Olduvai and Gauss Chrons is 42.8 m/m.y., and in the Gauss Chron it is 28.0 m/m.y. (Fig. F21). Magnetic polarity chrons were identified in Cores 191-1179C-19H through 23H, extending the magnetic stratigraphy of Hole 1179C from C3A down to the young end of C5Dr. The magnetic stratigraphy for Site 1179 thus consists of a complete record of virtually all the recognized polarity chrons from the mid-Miocene forward (Fig. F21).

The magnetization of the sediments in Cores 191-1179C-24H through 26X is predominantly normal polarity and could be from the Cretaceous normal superchron (121–83 Ma). If this interpretation is correct, there may be a hiatus between Cores 191-1179C-23H and 24H. Using accepted correlations between magnetic polarity and geologic time, the Miocene/Pliocene boundary is present in Section 191-1179C-15H-3 and the middle/late Miocene boundary is in Section 191-1179C-22H-6. Core 191-1179C-23H contains the deepest interpretable record

F20. Age-depth curve for Site 1179 developed from biostratigraphic data, p. 44.



F21. Age-depth curve for Site 1179 from interpretations of paleomagnetic data, p. 45.



and has the early/middle Miocene boundary in Section 5. The bottom of Core 191-1179C-23H has an age of ~17.6 Ma.

Using the magnetic polarity sequence, the sedimentation rate curve can be divided into three main segments with different slopes (Fig. F21). These three sections correspond to lithostratigraphic Units I, II, and III. Cores 191-1179C-22H and 23H, which consist of pelagic brown clay, display the slowest sedimentation rate (1.56 m/m.y.) for the upper part of Unit III. Sedimentation rates increase upward. Unit II, which spans Cores 191-1179C-22H through 20H, has a sedimentation rate of 7.56 m/m.y. For Unit I, the rate is 29.29 m/m.y. The curve implies either that Site 1179 drifted into an area of increased productivity in the late Miocene and Pliocene or that oceanographic conditions changed in such a way as to lead to a 20-fold increase in sediment accumulation.

Samples from the basaltic basement section of Hole 1179D give mainly negative inclinations consistent with reversed magnetic polarity at a site north of the equator. Reversed polarity was expected because the site is located on magnetic Anomaly M8. A preliminary paleolatitude for the basalt samples is  $4.2^\circ \pm 9.9^\circ$ .

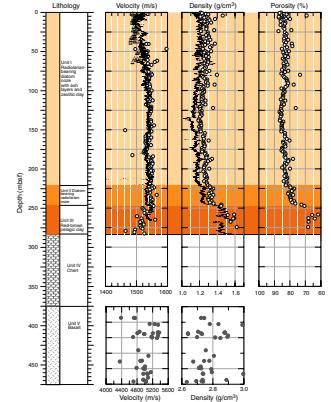
### Physical Properties

Measured physical properties of sediments recovered at Site 1179 correlate well with lithostratigraphy. *P*-wave velocities in the sediments are typically 1530–1550 m/s. Average densities range from 1.265 to 1.450 g/cm<sup>3</sup>, and average porosities range from 67% to 83% (Fig. F22). Average densities and velocities in the basalts are 2.745 g/cm<sup>3</sup> and 5002 m/s, respectively. Within Unit I, bulk density, thermal conductivity, and natural gamma radiation decrease with depth in the upper 150 m of the section and porosity increases to >85%. We suspect that these seemingly paradoxical trends in density and porosity are caused by a progressive increase in the relative abundance of diatom fragments, which have low grain densities and contain large volumes of intragranular pore space. The contact between Units I and II is marked by small changes in physical properties, but the transition from Unit II to the pelagic clays of Unit III is dramatic. Densities increase, porosities fall to <70%, and there are marked increases in natural gamma radiation and magnetic susceptibility. Marked changes in natural gamma radiation and magnetic susceptibility at a depth of ~265 mbsf also suggest a compositional change within Unit III.

### Downhole Logging

Wireline logging data acquisition was limited to one tool string (the triple combo) and to depths of <300 mbsf, owing to bridging of the hole. The caliper data from 5777 to 5820 mbrf showed hole diameters ranging from 7 to 16 in. On most logging runs, the caliper remained fully opened (16.5 in). The triple-combo measurements (particularly the APS) are affected by the large hole size; furthermore, the HLDT developed a functioning problem so the density and porosity data should be treated cautiously. The DIT data clearly recorded the lithologic change between lithostratigraphic Units II and III, marked by an increase in the electrical resistivity at 243 mbsf. The boundary between Units III and IV is marked by a strong increase in resistivity (from 0.7 to 3.5 Ωm). The chert layers consist of alternating high-resistivity layers (nodules) and interbedded low-resistivity (clay rich) layers. The data from the MGT are well correlated with total natural gamma counts

F22. Summary figure showing velocity, density, and porosity vs. depth at Site 1179, p. 46.



from the HLDT and present much higher vertical resolution and better defined layer boundaries. Gamma-ray measurements responded to the presence of ash layers in the uppermost part of the logged section. The DSA tool was deployed successfully on Cores 191-1179C-4H and 7H. The maximum pressure recorded by the tool was ~9000 psi, and shocks did not exceed 2.7 g. Plots of acceleration data clearly show downhole heave and significant events during core-barrel hole penetration and recovery.

### **Microbiology**

Sediment samples from Holes 1179B and 1179C were collected to characterize both the chemistry and microbial activity in this environment. Microbial activity will be inferred from incubation experiments and from shore-based lipid analysis. Four whole-round cores (WRCs) were collected from different depths (5, 30, 100, and 200 mbsf) for incubation experiments. In addition, a more extensive set of WRCs were collected at depths ranging from 0.05 to 278.12 mbsf for detailed analyses of bacterial lipid changes with depth. As certain cell-membrane lipids are diagnostic of particular groups of bacteria, the lipid analyses may reveal the presence of different types of bacteria throughout the sedimentary column. Interstitial pore waters were collected for chemical analyses from the same approximate depths taken for lipids in order to relate the microbial communities to the geochemical sedimentary environment. Whole rounds cut on the catwalk were also sampled on several occasions for PFT contamination tests.

## REFERENCES

- Berggren, W.A., Kent, D.V., Swisher, C.C., III, and Aubry, M.-P., 1995. A revised Cenozoic geochronology and chronostratigraphy. *In* Berggren, W.A., Kent, D.V., Aubry, M.-P., and Hardenbol, J. (Eds.), *Geochronology, Time Scales and Global Stratigraphic Correlation*. Spec. Publ.—Soc. Econ. Paleontol. Mineral. (Soc. Sediment. Geol.), 54:129–212.
- Butler, R., and Duennebie, F.K., 1987. Teleseismic observations from OSS IV. *In* Duennebie, F.K., Stephen, R., Gettrust, J.F., et al., *Init. Repts. DSDP*, 88: Washington (U.S. Govt. Printing Office), 147–153.
- Carlson, R.L., Gangi, A.F., and Snow, K.R., 1986. Empirical reflection travel time versus depth and velocity versus depth functions for the deep-sea sediment column. *J. Geophys. Res.*, 91:8249–8266.
- Dixon, T.H., and Stern, R.J., 1983. Petrology, chemistry, and isotopic compositions of submarine volcanoes in the southern Mariana arc. *Geol. Soc. Am. Bull.*, 94:1159–1172.
- Duennebie, F.K., 1987. The 26 May 1983 Japan earthquake recorded by OSS IV. *In* Duennebie, F.K., Stephen, R., Gettrust, J.F., et al., *Init. Repts. DSDP*, 88: Washington (U.S. Govt. Printing Office), 155–165.
- Duennebie, F.K., McCreery, C.S., Harris, D., Cessaro, R.K., Fisher, C., and Anderson, P., 1987a. OSS IV: noise levels, signal-to-noise ratios, and noise sources. *In* Duennebie, F.K., Stephen, R., Gettrust, J.F., et al., *Init. Repts. DSDP*, 88: Washington (U.S. Govt. Printing Office), 89–103.
- Duennebie, F.K., Stephen, R., Gettrust, J.F., et al., 1987b. *Init. Repts. DSDP*, 88: Washington (U.S. Govt. Printing Office).
- Fischer, A.G., Heezen, B.C., et al., 1971. *Init. Repts. DSDP*, 6: Washington (U.S. Govt. Printing Office).
- Fukao, Y., 1992. Seismic tomogram of the Earth's mantle: geodynamic implications. *Science*, 258:625–630.
- Gradstein, F.M., Agterberg, F.P., Ogg, J.G., Hardenbol, J., van Veen, P., Thierry, J., and Huang, Z., 1994. A Mesozoic time scale. *J. Geophys. Res.*, 99:24051–24074.
- , 1995. A Triassic, Jurassic and Cretaceous time scale. *In* Berggren, W.A., Kent, D.V., Aubry, M.-P., and Hardenbol, J. (Eds.), *Geochronology, Time Scales and Global Stratigraphic Correlation*. Spec. Publ.—Soc. Econ. Paleontol. Mineral., 54:95–126.
- Heath, G.R., Burckle, L.H., et al., 1985. *Init. Repts. DSDP*, 86: Washington (U.S. Govt. Printing Office).
- Heezen, B.C., MacGregor, I.D., et al., 1973. *Init. Repts. DSDP*, 20: Washington (U.S. Govt. Printing Office).
- Hussong, D.M., and Uyeda, S., 1982. Tectonic processes and the history of the Mariana Arc: a synthesis of the results of Deep Sea Drilling Project Leg 60. *In* Hussong, D.M., Uyeda, S., et al., *Init. Repts. DSDP*, 60: Washington (U.S. Govt. Printing Office), 909–929.
- Ingle, J.C., Jr., Suyehiro, K., von Breymann, M.T., et al., 1990. *Proc. ODP, Init. Repts.*, 128: College Station, TX (Ocean Drilling Program).
- JOI-ESF, 1987. Report of the Second Conference on Scientific Ocean Drilling. Washington (JOI, Inc.).
- JOI/USSAC, 1994. BOREHOLE: a plan to advance post-drilling sub-seafloor science. *JOI/USSAC Workshop Rep.*, Univ. Miami, FL, 1–83.
- Kanazawa, T., Suyehiro, K., Hirata, N., and Shinohara, M., 1992. Performance of the ocean broadband downhole seismometer at Site 794. *In* Tamaki, K., Suyehiro, K., Allan, J., McWilliams, M., et al., *Proc. ODP, Sci. Results*, 127/128 (Pt. 2): College Station, TX (Ocean Drilling Program), 1157–1171.
- Karig, D.E., 1975. Basin genesis in the Philippine Sea. *In* Karig, D.E., Ingle, J.C., Jr., et al., *Init. Repts. DSDP*, 31: Washington (U.S. Govt. Printing Office), 857–879.

- Larson, R.L., and Chase, C.G., 1972. Late Mesozoic evolution of the western Pacific Ocean. *Geol. Soc. Am. Bull.*, 83:3637–3644.
- Larson, R.L., and Lowrie, W., 1975. Paleomagnetic evidence for motion of the Pacific plate from Leg 32 basalts and magnetic anomalies. In Larson, R.L., and Moberly, R., et al., *Init. Repts. DSDP*, 32: Washington (U.S. Govt. Printing Office), 571–577.
- Larson, R.L., Moberly, R., et al., 1975. *Init. Repts. DSDP*, 32: Washington (U.S. Govt. Printing Office).
- Larson, R.L., Steiner, M.B., Erba, E., and Lancelot, Y., 1992. Paleolatitudes and tectonic reconstructions of the oldest portion of the Pacific Plate: a comparative study. In Larson, R.L., Lancelot, Y., et al., *Proc. ODP, Sci. Results*, 129: College Station, TX (Ocean Drilling Program), 615–631.
- Ludwig, W.J., and Houtz, R.E., 1979. Isopach map of sediments in the Pacific Ocean Basin and marginal sea basins. *AAPG Map Ser.*, 647.
- Montagner, J.P., Karczewski, J.F., Romanowicz, B., Bouaricha, S., Lognonne, P., Roullet, G., Stutzmann, E., Thiriot, J.L., Brion, J., Dole, B., Fouassier, D., Koenig, J.C., Savary, J., Floury, L., Dupond, J., Echardour, A., Floc'h, H., 1994. The French pilot experiment OFM-SISMOBS: first scientific results on noise level and event detection. *Phys. Earth Planet. Int.*, 84:321–336.
- Montagner, J.-P., and Lancelot, Y. (Eds.), 1995. Multidisciplinary observatories on the deep seafloor. *INSU/CNRS, IFREMER, ODP-France, OSN/USSAC, ODP-Japan*.
- Nakanishi, M., Sager, W.W., and Klaus, A., 1999. Magnetic lineations within Shatsky Rise, northwest Pacific Ocean: implications for hot spot–triple junction interaction and oceanic plateau formation. *J. Geophys. Res.*, 104:7539–7556.
- Nakanishi, M., Tamaki, K., and Kobayashi, K., 1989. Mesozoic magnetic anomaly lineations and seafloor spreading history of the Northwestern Pacific. *J. Geophys. Res.*, 94:15437–15462.
- Ocean Drilling Program, 1996. *Understanding Our Dynamic Earth through Ocean Drilling: Ocean Drilling Program Long Range Plan Into the 21st Century*: Washington (Joint Oceanographic Institutions).
- Pettigrew, T.L., Casey, J.F., Miller, D.J., et al., 1999. *Proc. ODP, Init. Repts.*, 179 [CD-ROM]. Available from: Ocean Drilling Program, Texas A&M University, College Station, TX 77845-9547, USA.
- Plank, T., Ludden, J.N., Escutia, C., et al., 2000. *Proc. ODP, Init. Repts.*, 185 [CD-ROM]. Available from: Ocean Drilling Program, Texas A&M University, College Station TX 77845-9547, USA.
- Purdy, G.M., and Dziewonski, A.M., 1988. *Proc. of a Workshop on Broadband Downhole Seismometers in the Deep Ocean*. Joint Oceanogr. Inst. and U.S. Sci. Advisory Comm.
- Sacks, I.S., Suyehiro, K., Acton, G.D., et al., 2000. *Proc. ODP, Init. Repts.*, 186 [CD-ROM]. Available from: Ocean Drilling Program, Texas A&M University, College Station, TX 77845-9547, USA.
- Sager, W.W., and Han, H.-C., 1993. Rapid formation of the Shatsky Rise oceanic plateau inferred from its magnetic anomaly. *Nature*, 364:610–613.
- Sager, W.W., Handschumacher, D.W., Hilde, T.W.C., and Bracey, D.R., 1988. Tectonic evolution of the northern Pacific Plate and Pacific-Farallon-Izanagi triple junction in the Late Jurassic and Early Cretaceous (M21–M10). *Tectonophysics*, 155:345–364.
- Sager, W.W., Kim, J., Klaus, A., Nakanishi, M., and Khankishieva, L.M., 1999. Bathymetry of Shatsky Rise, northwest Pacific Ocean: implications for ocean plateau development at a triple junction. *J. Geophys. Res.*, 104:7557–7576.
- Sliter, W.V., and Brown, G.R., 1993. Shatsky Rise: seismic stratigraphy and sedimentary record of Pacific paleoceanography since the Early Cretaceous. In Natland, J.H., Storms, M.A., et al., *Proc. ODP, Sci. Results*, 132: College Station, TX (Ocean Drilling Program), 3–13.
- Smith, W.H.F., and Sandwell, D.T., 1997. Global seafloor topography from satellite altimetry and ship depth soundings. *Science*, 277:1956–1962.
- Stephen, R.A., Collins, J.A., and Peal, K.R., 1999. Seafloor seismic stations perform well. *Eos*, 80:592.

- Stern, R.J., Bloomer, S.H., Lin, P.-N., and Smoot, N.C., 1989. Submarine arc volcanism in the southern Mariana arc as an ophiolite analogue. *Tectonophysics*, 168:151–170.
- Su, W.-J., Woodward, R.L., and Dziewonski, A.M., 1992. Deep origin of mid-ocean-ridge velocity anomalies. *Nature*, 360:149–152.
- Suyehiro, K., Kanazawa, T., Hirata, N., and Shinohara, M., 1995. Ocean downhole seismic project. *J. Phys. Earth*, 43:599–618.
- Suyehiro, K., Kanazawa, T., Hirata, N., Shinohara, M., and Kinoshita, H., 1992. Broadband downhole digital seismometer experiment at Site 794: a technical paper. In Tamaki, K., Suyehiro, K., Allan, J., McWilliams, M., et al., *Proc. ODP, Sci. Results*, 127/128 (Pt. 2): College Station, TX (Ocean Drilling Program), 1061–1073.
- Tanimoto, T., 1988. The 3-D shear wave structure in the mantle by overtone waveform inversion, II: inversion of X-waves, R-waves, and G-waves. *J. Geophys.*, 93:321–333.
- van der Hilst, H., Engdahl, R., Spakman, W., and Nolet, G., 1991. Tomographic imaging of subducted lithosphere below northwest Pacific island arcs. *Nature*, 353:37–43.
- Zhang, Y.S., and Tanimoto, T., 1992. Ridges, hotspots and their interaction as observed in seismic velocity maps. *Nature*, 355:45–49.

**Figure F1.** Location map of seismic station coverage in the northwest Pacific. Solid circles = land seismic stations, open circles = current (Sites 1150, 1151, and 1179) and proposed (Site WP-1) seafloor borehole observatories, and the shaded circle = a presently inactive land seismic station (at HCH). Note that the few borehole stations effectively complement and expand the existing network. YSS = Yuzhno Sakhalinsk, Russia; NMR = Nemuro, Japan; HCH = Hachijojima, Japan; PHN = Pohang, Korea; OGS = Chichijima, Japan; MCSJ = Minami-torishima, Japan; ISG = Ishigakijima, Japan; TGY = Tagaytay, Philippines; PATS = Ponphei, Micronesia; PMG = Port Moresby, Papua New Guinea.

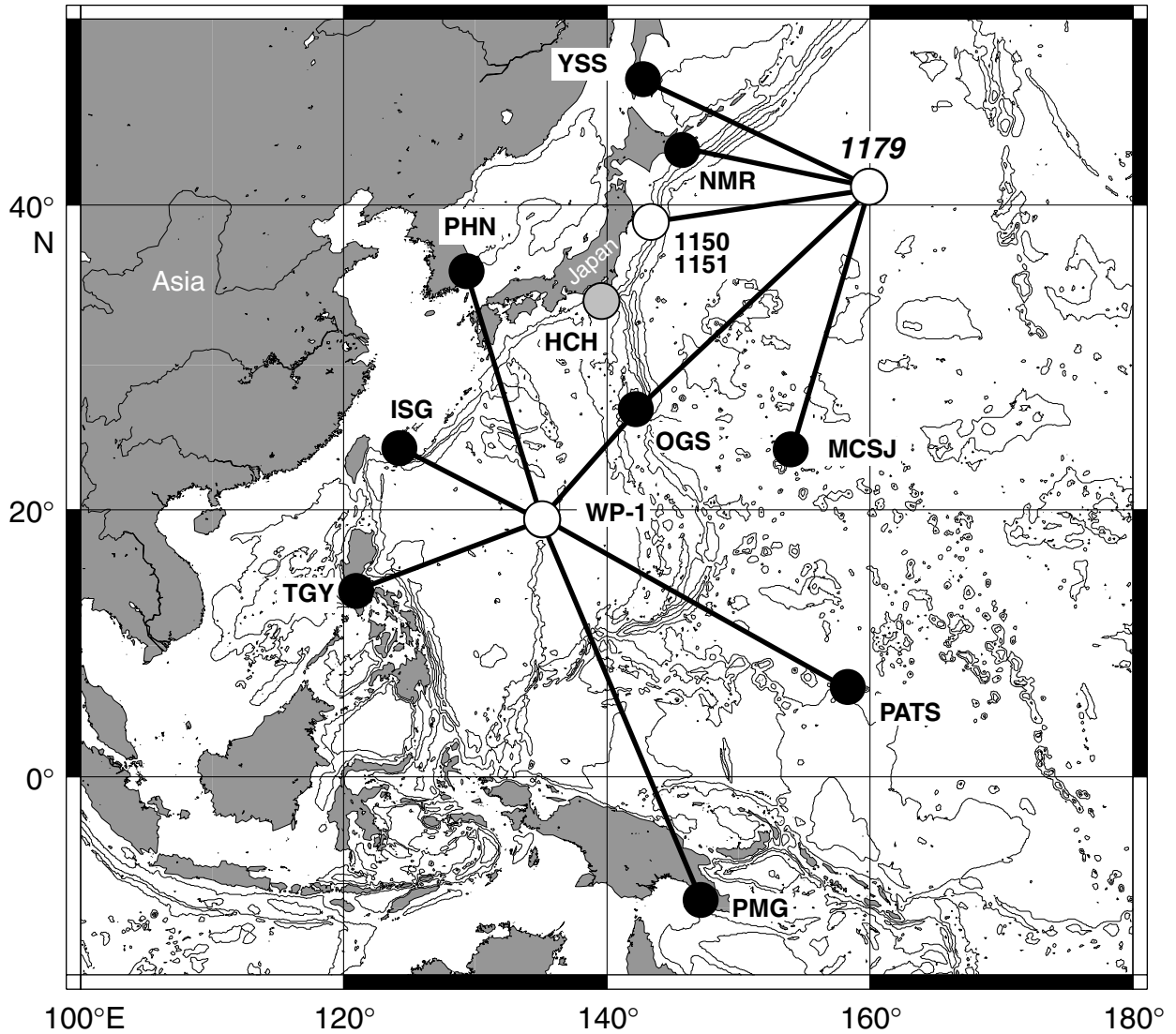


Figure F2. Location of Site 1179 relative to circum-Pacific and other earthquakes for the period 1992–1996. Distances from Site 1179 are shown (thick lines) in 5000-km intervals. M = earthquake magnitude.

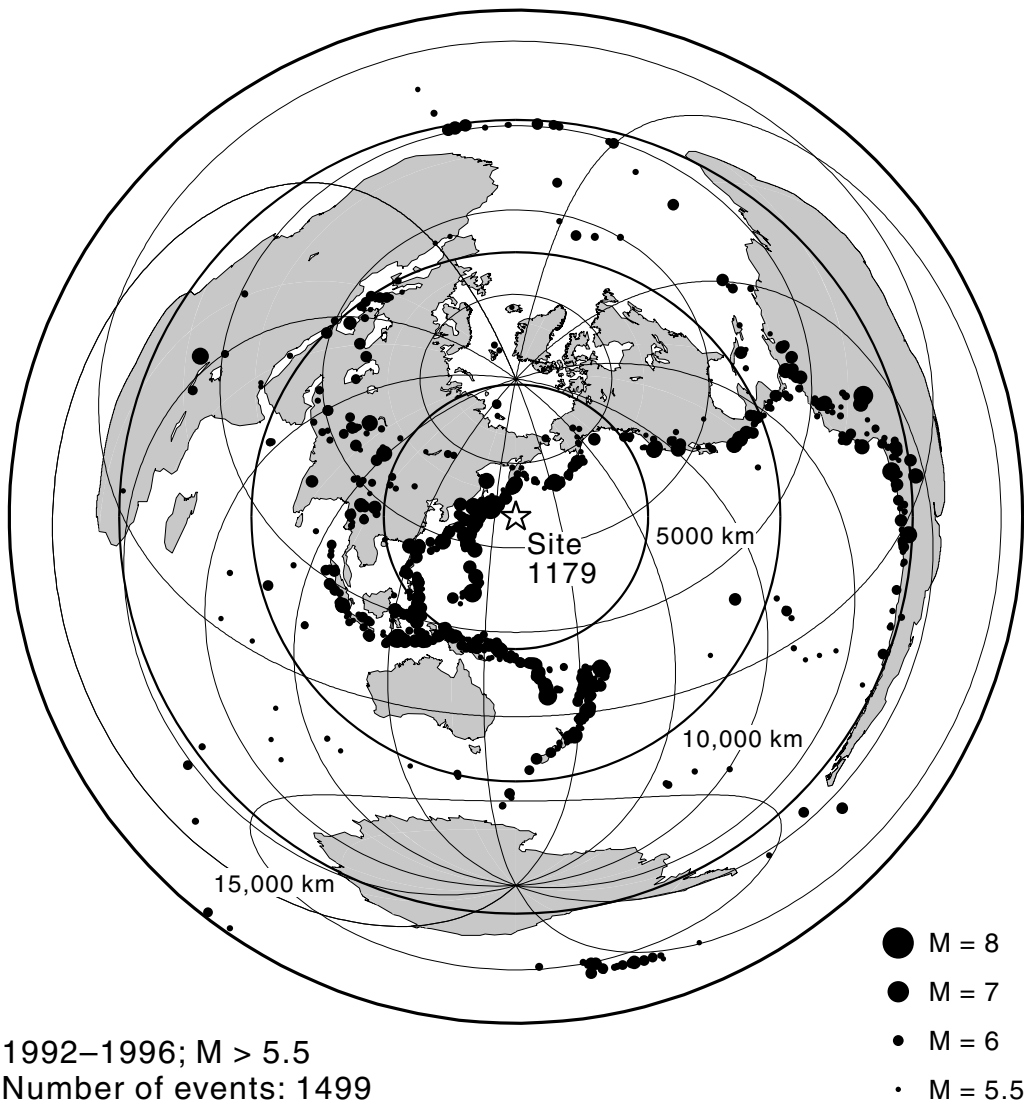


Figure F3. Locations of Leg 191 drill sites and magnetic lineations in the northwest Pacific. The map shows predicted bathymetry (Smith and Sandwell, 1997) and magnetic lineations (Nakanishi et al., 1989). Sites 1180/1181 and 1182 are the hard-rock reentry system test sites.

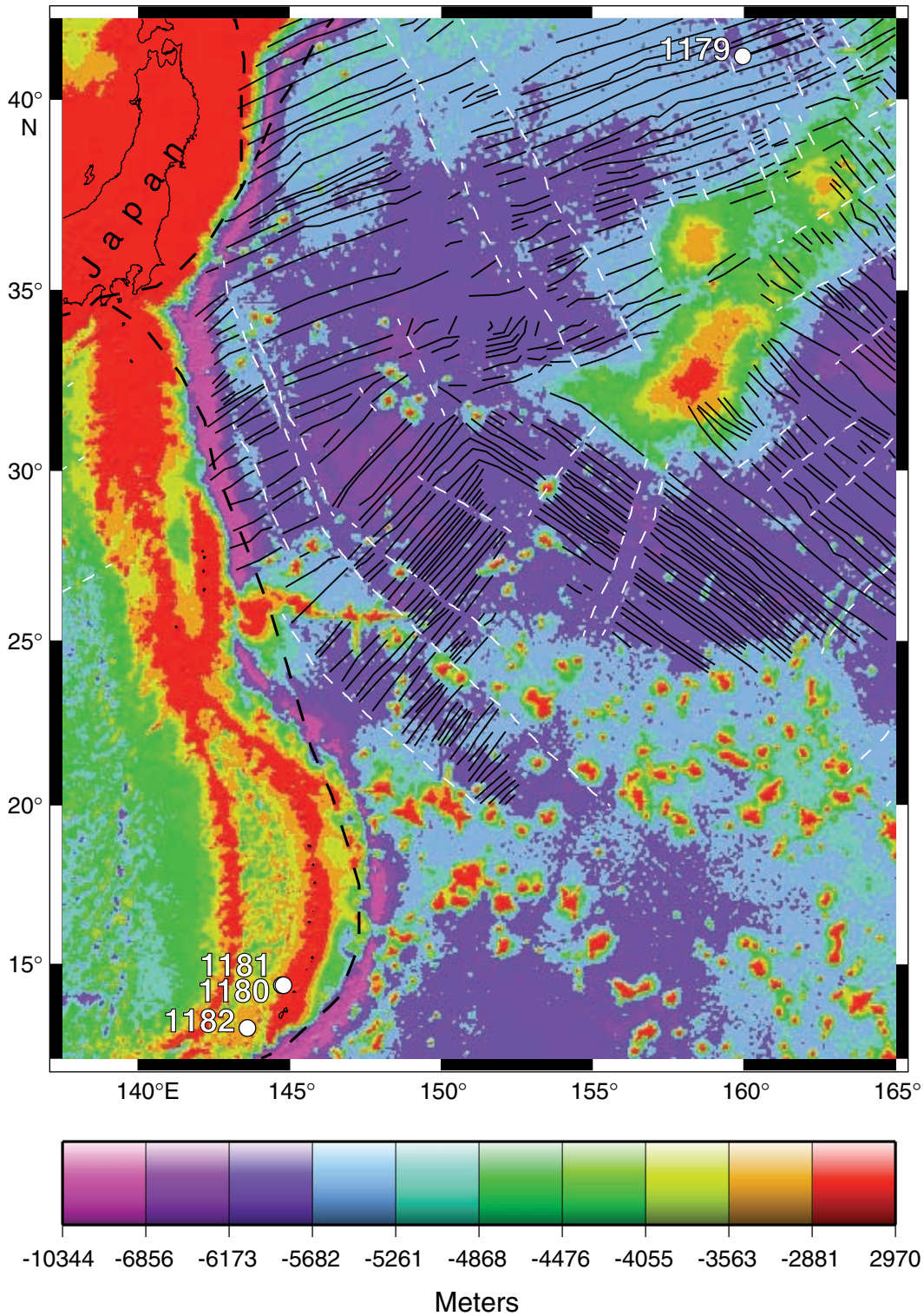
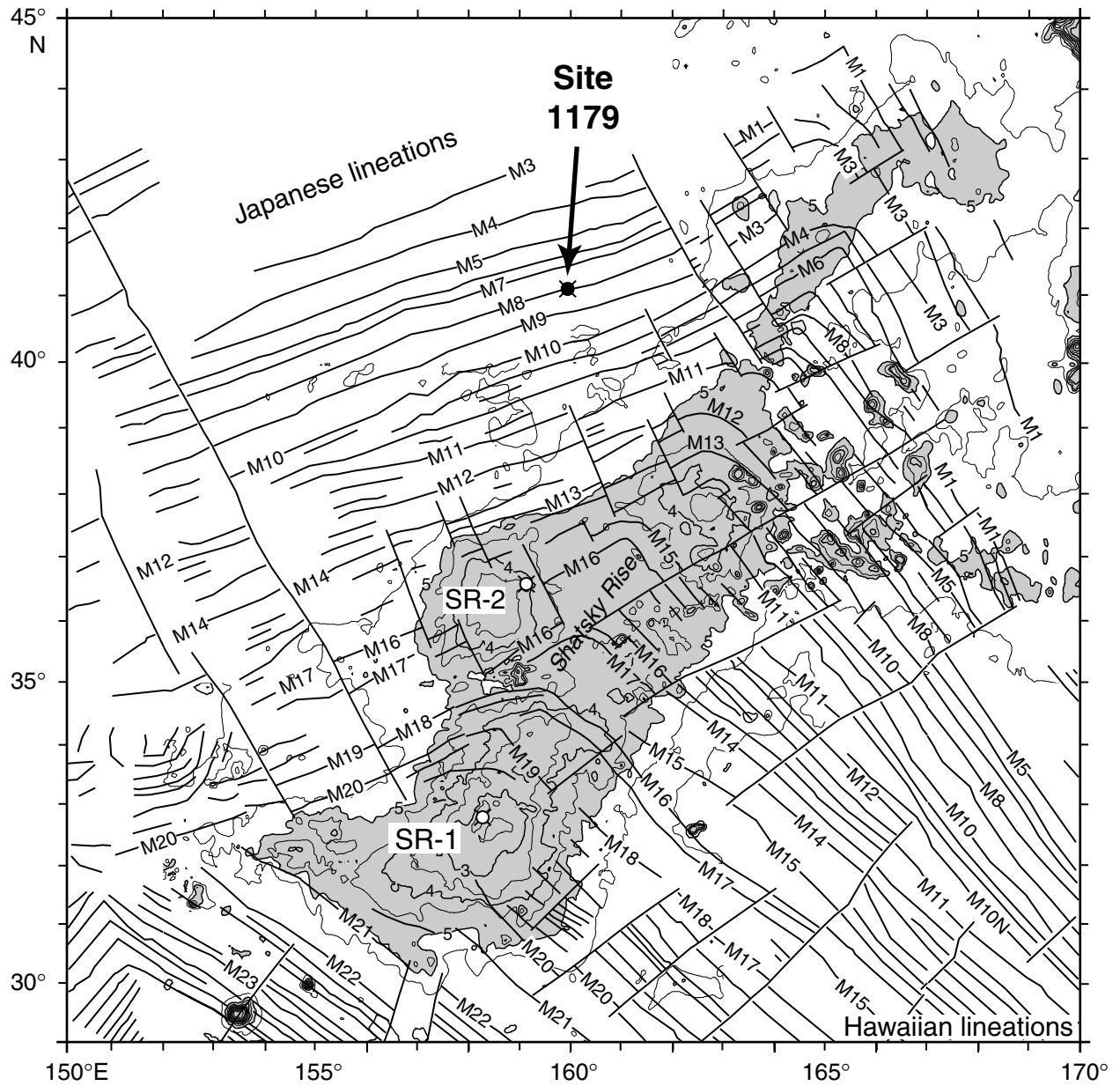


Figure F4. Site 1179 location relative to magnetic lineations in the northwest Pacific. Thick lines show magnetic lineations and fracture zones. Thin lines show 500-m bathymetry contours (from Sager et al., 1999; Nakanishi et al., 1989). Proposed Sites SR-1 and SR-2 (open circles) are the proposed hard-rock reentry system test sites on Shatsky Rise (shaded region).



**Figure F5.** Comparison of stratigraphic columns at Site 1179 and other DSDP and ODP boreholes in the northwest Pacific. The numbers at the top give site designations. Biostratigraphic ages are along the left side of each column. The distance from Site 1179 is shown at the bottom.

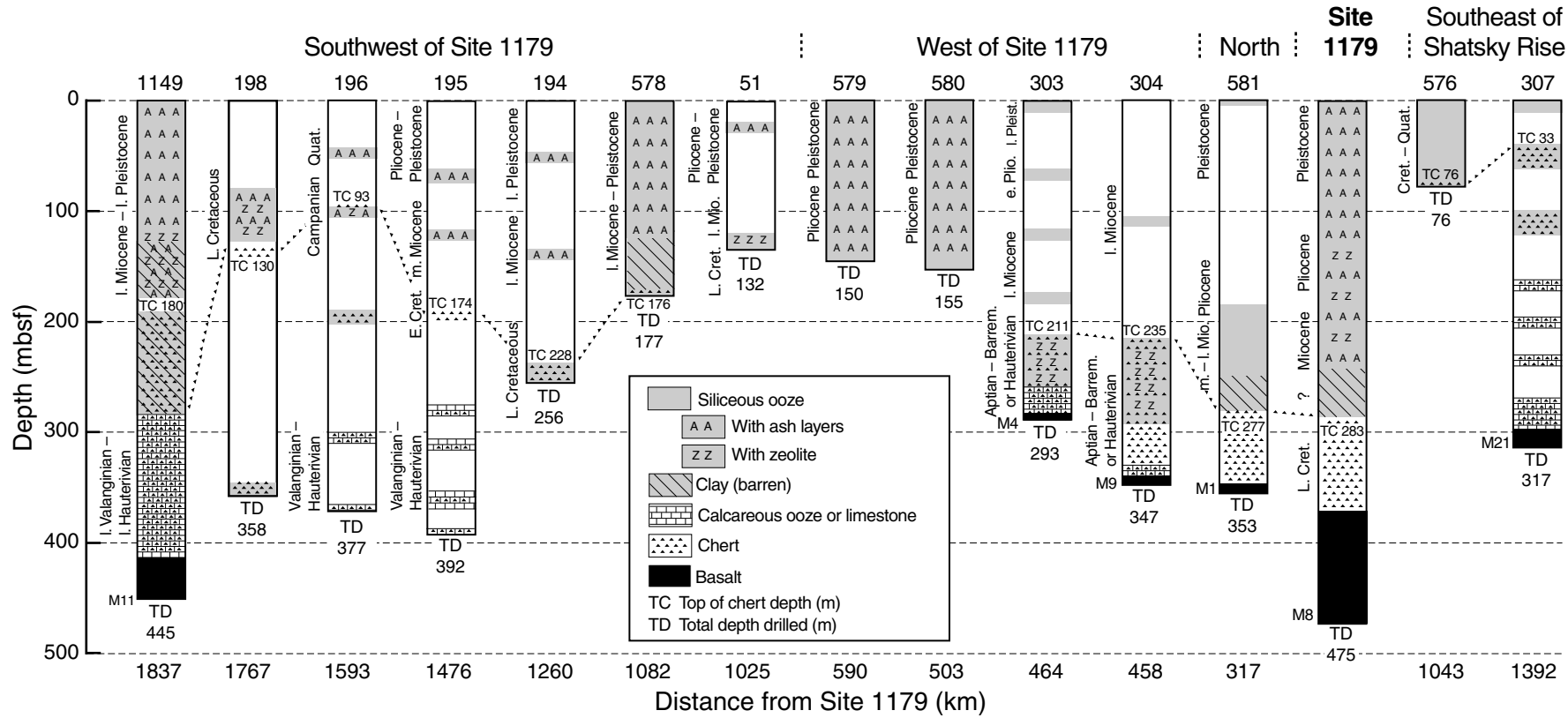
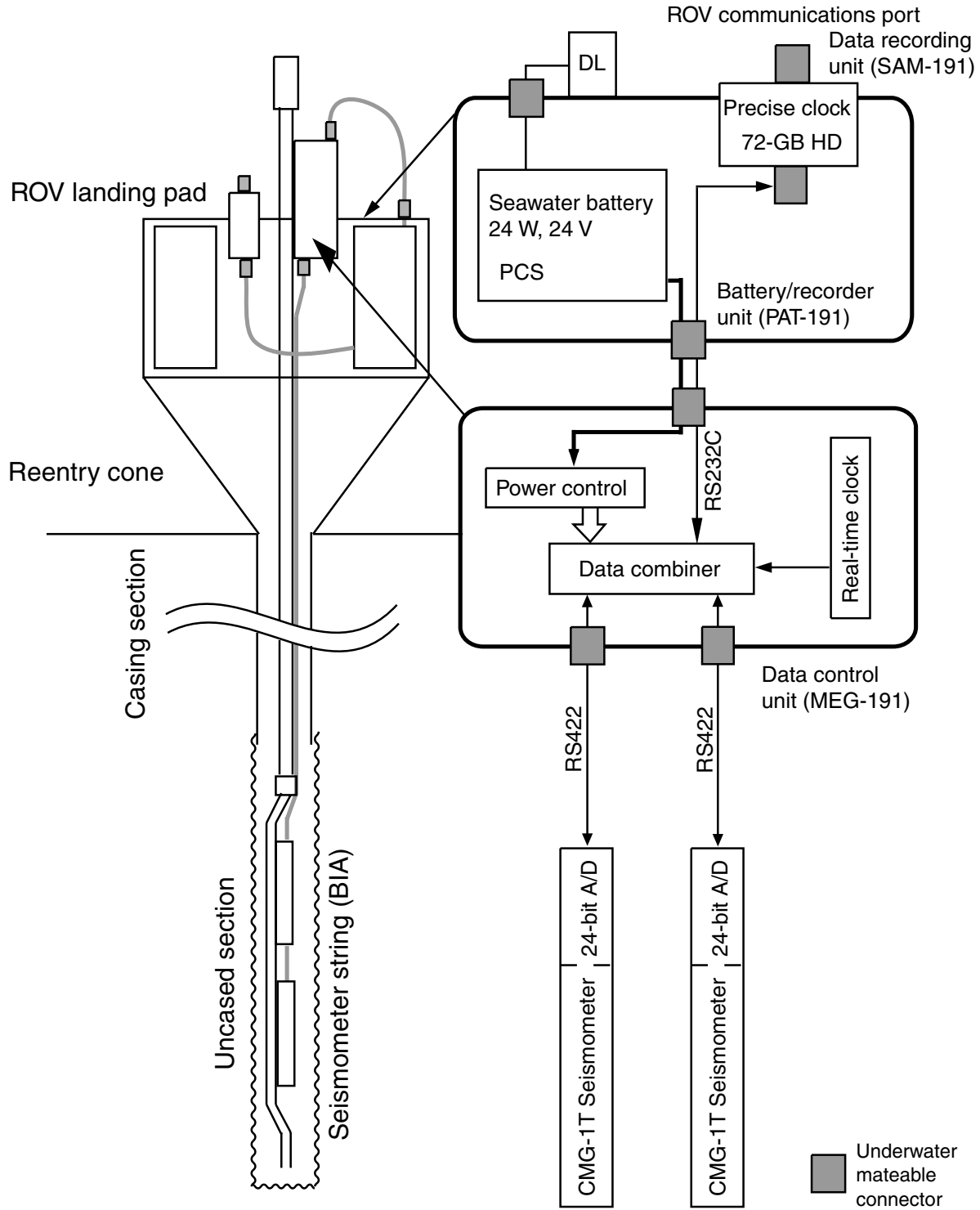


Figure F6. Schematic of the WP-2 seismic borehole observatory. PCS = power control system, ROV = remotely operated vehicle, DL = data logger, HD = hard drive, BIA = borehole instrument assembly, MEG = multiple-access expandable gateway, SAM = storage acquisition module, PAT = power access terminal.



**Figure F7.** Multiple-access expandable gateway (MEG-191) system controller attached to the riser/hanger assembly prior to installation.



**Figure F8.** Power access terminal (PAT) battery frame being lowered through the moonpool. The PAT was hung on the logging line by a bridle assembly consisting of wire cables, nylon straps, three glass ball floats, and a redundant acoustic release.

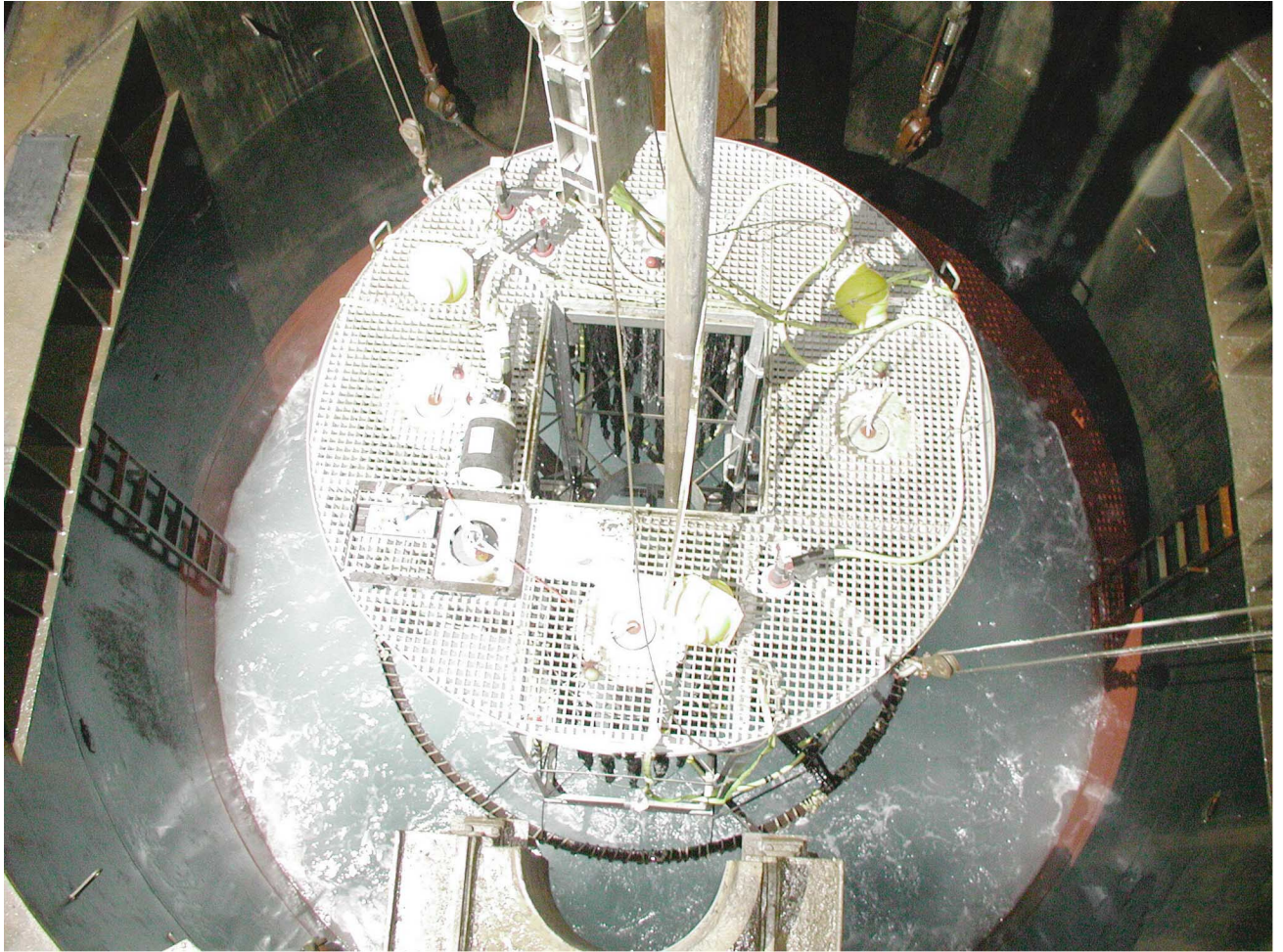


**Figure F9.** Snapshot from the VIT/subsea TV camera showing the PAT landed properly on top of the Hole 1179E reentry cone.



Figure F10. Schematic of the borehole seismic observatory installation in Hole 1179E. MEG = multiple-access expandable gateway, ROV = remotely operated vehicle, PAT = power access terminal.

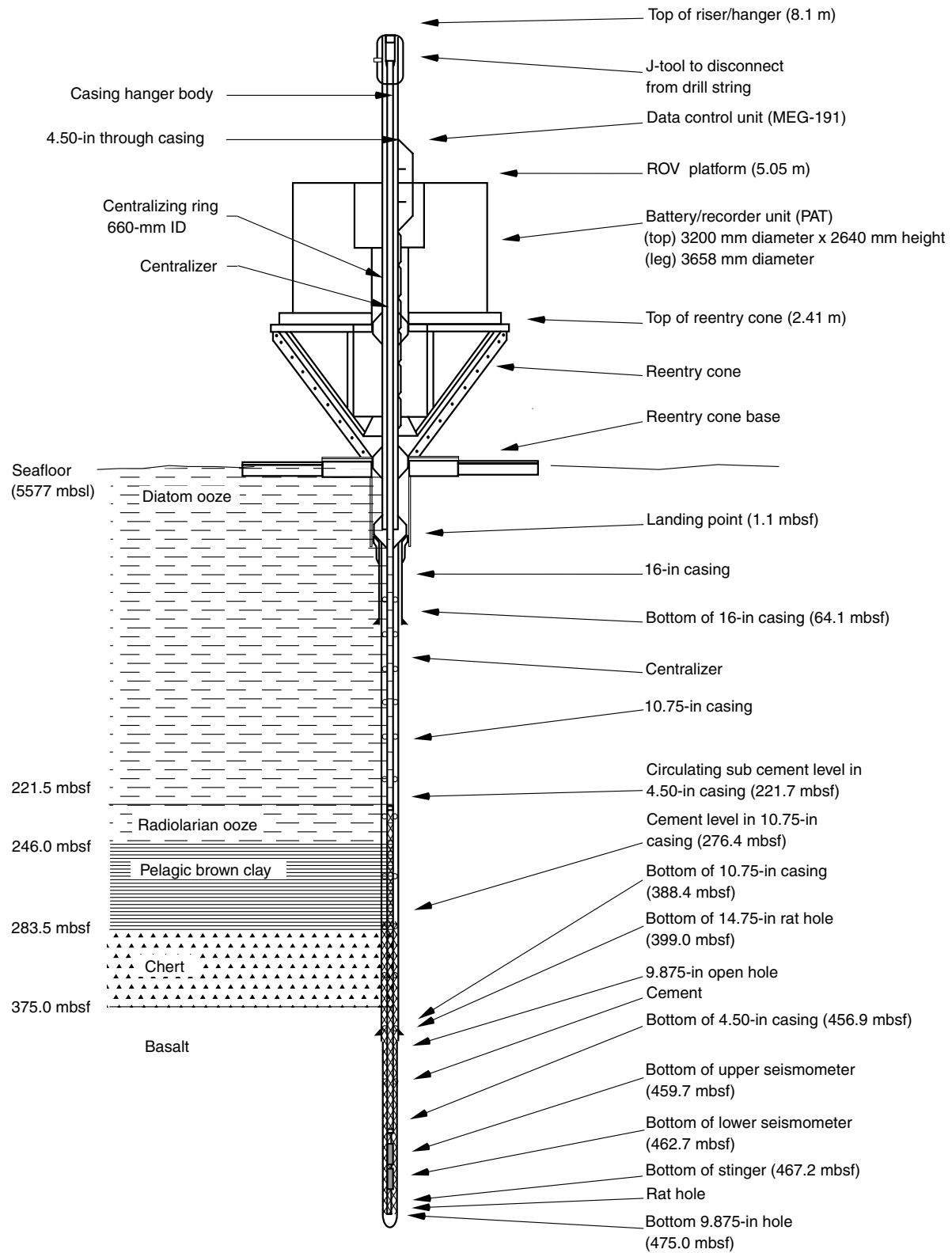
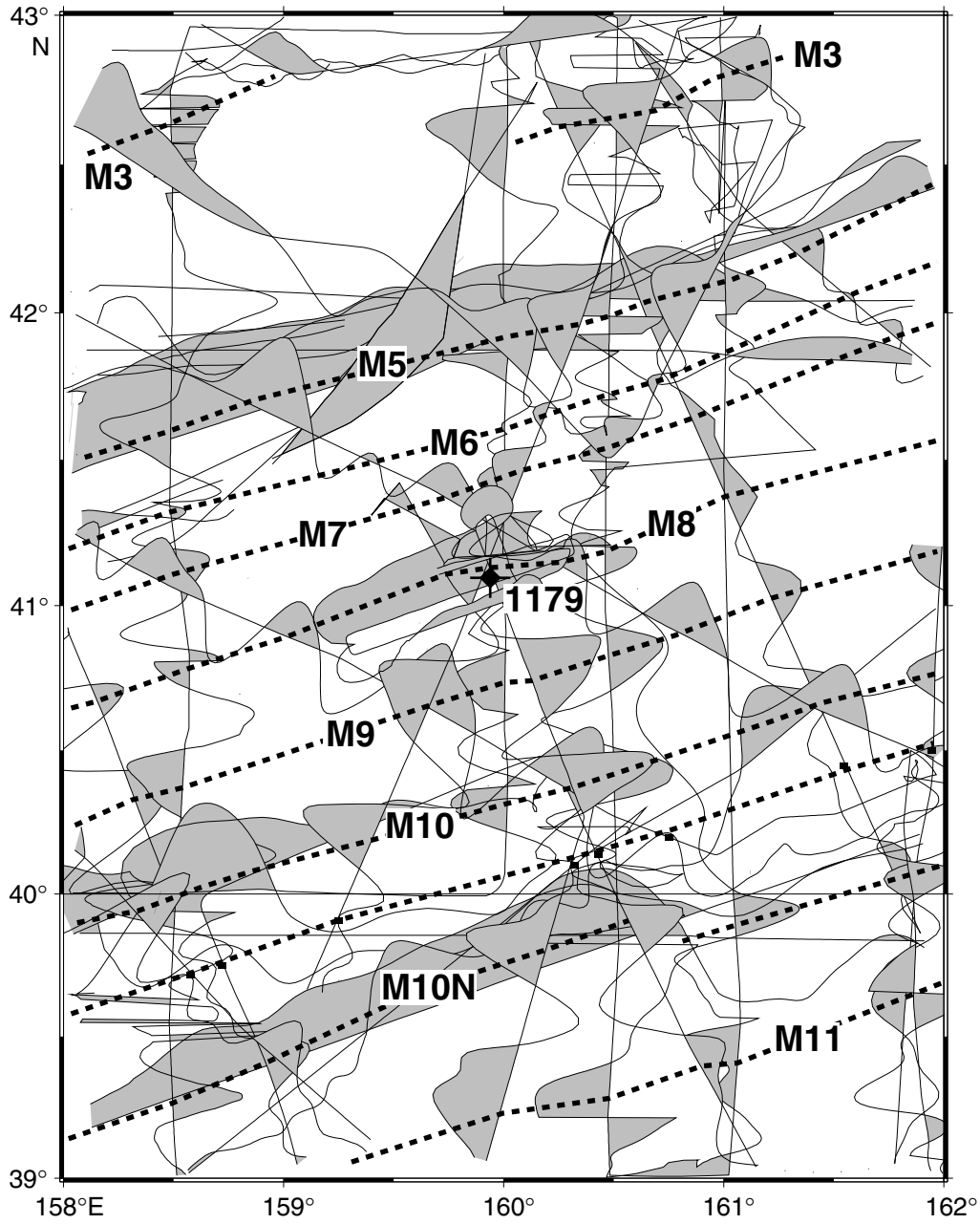


Figure F11. Magnetic lineations in the vicinity of Site 1179. Thin curved lines show magnetic anomalies, which are shaded where positive. Anomaly identifications are after Nakanishi et al. (1999). The location of Site 1179 is shown by the cross at the center of the figure. Dashed lines = magnetic lineation correlations.



**Figure F12.** Lithostratigraphic summary column for Site 1179. Core recovery is shown in left columns, with solid blocks indicating the amount of recovered core. Lithology and lithostratigraphic unit columns show generalized stratigraphy. Lightly shaded bands in Unit I lithology denote ash layers. Color reflectance, magnetic susceptibility, and natural gamma-ray columns show data measured on the archive multisensor track (color reflectance) and multisensor track (others). Curves in the far right column are from downhole logs. Magnetic polarity is shown by black (normal polarity) and white (reversed polarity) bands. Chron age designations are given next to the polarity column. **(Figure shown on next three pages.)**

Figure F12 (continued). (Caption shown on previous page.)

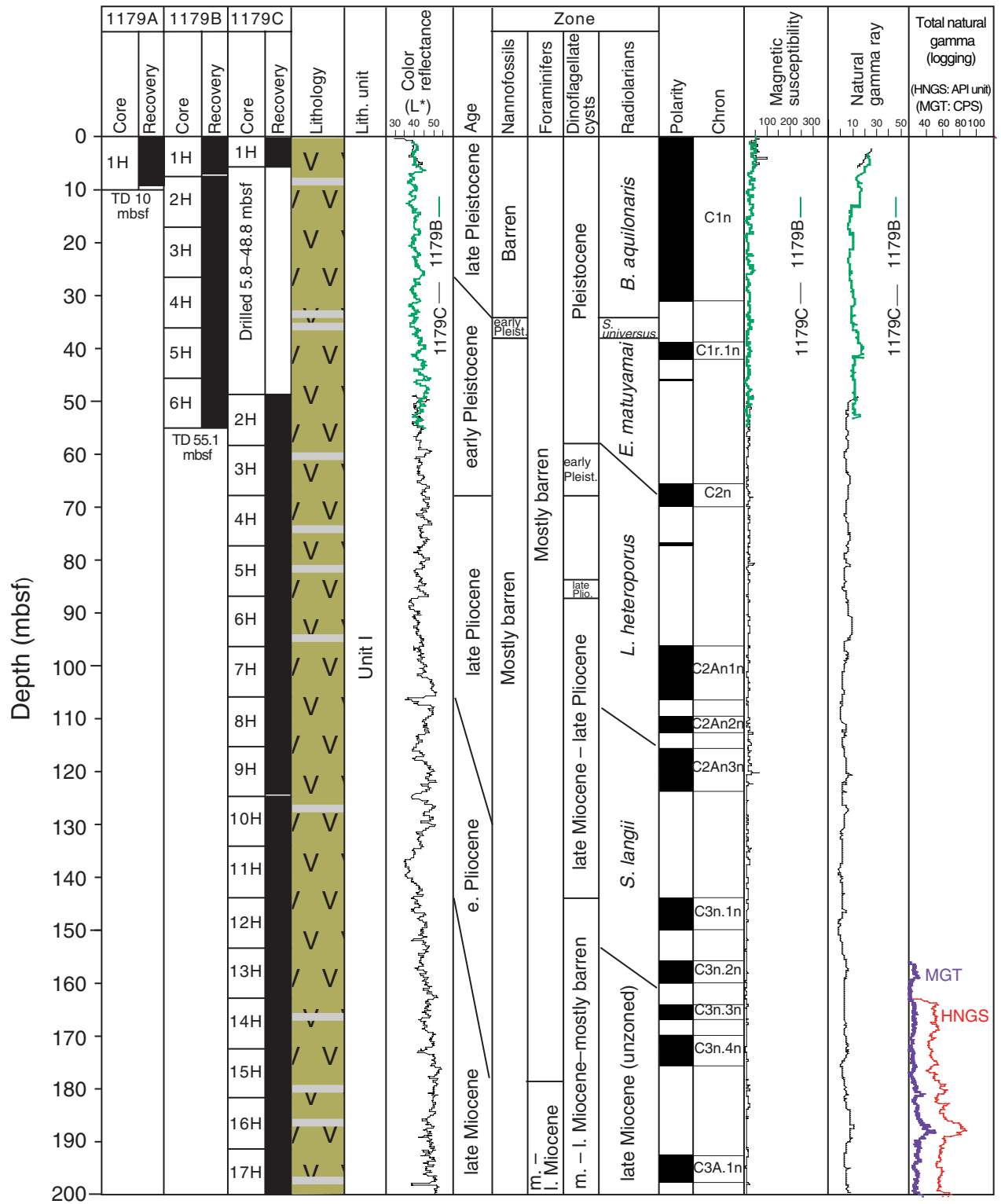


Figure F12 (continued).

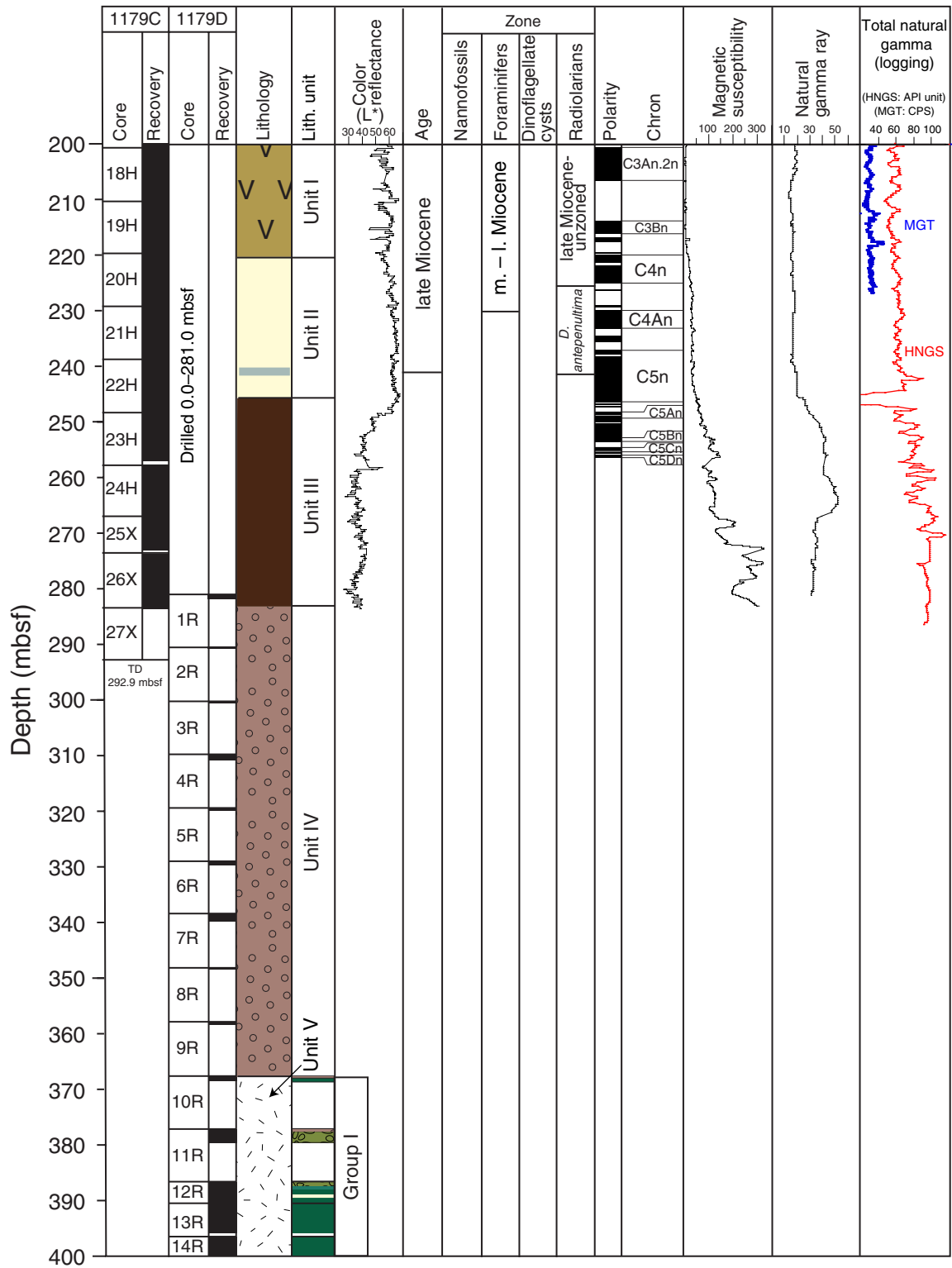
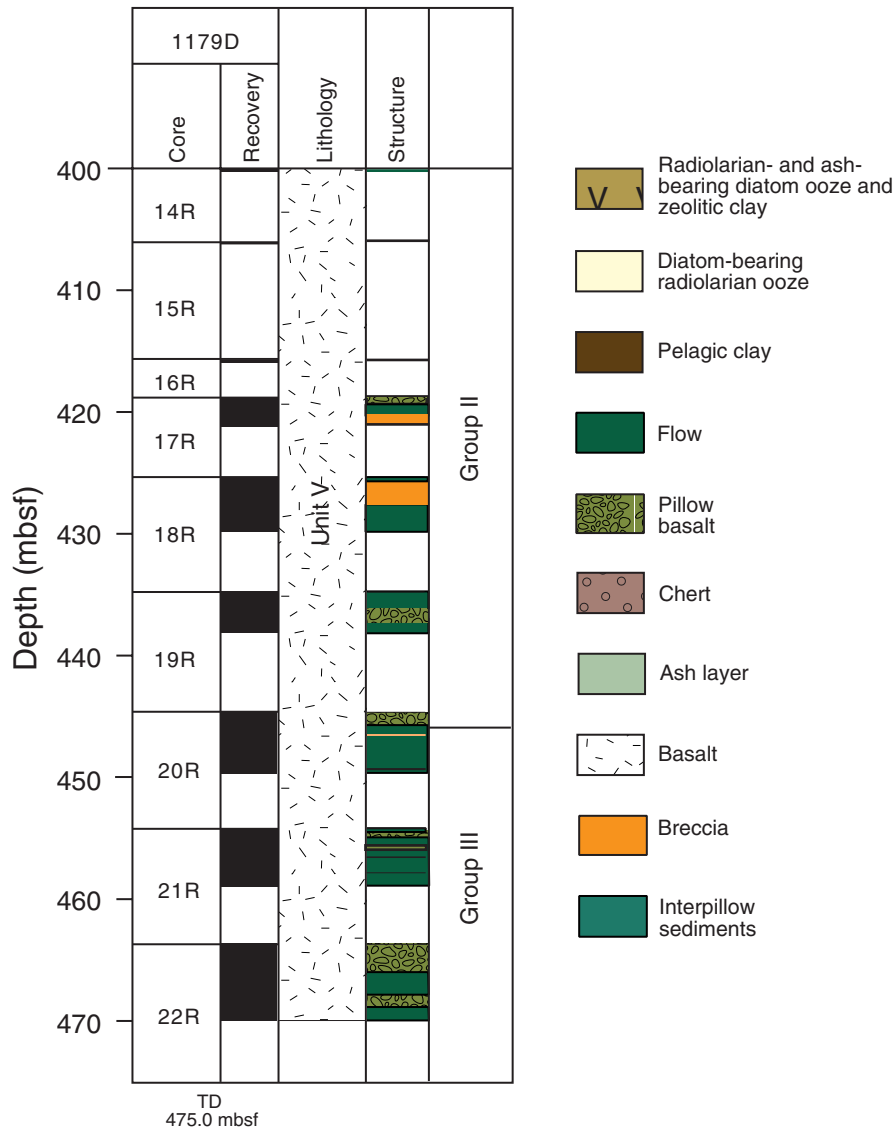
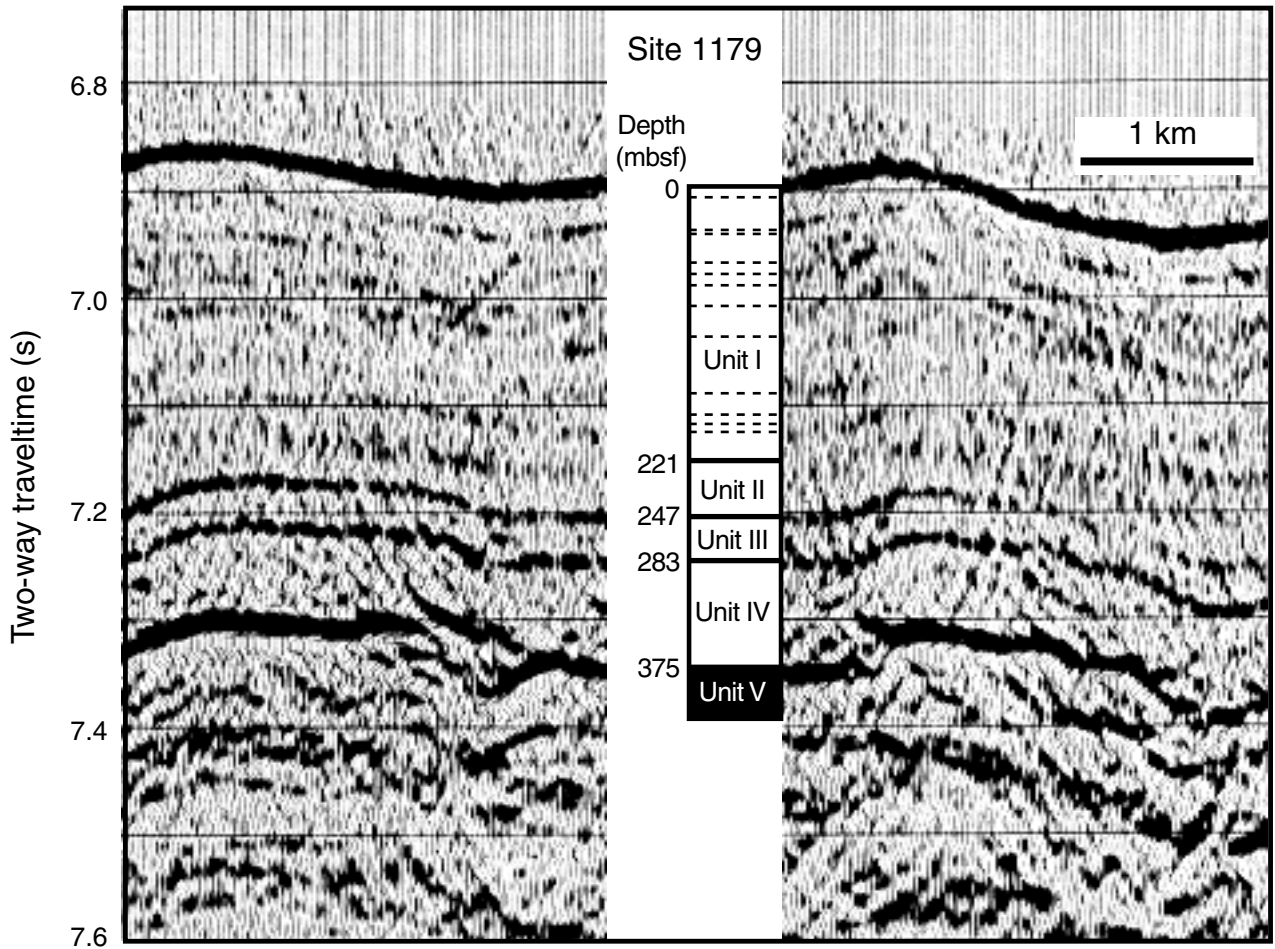


Figure F12 (continued).



**Figure F13.** Comparison of the multichannel seismic reflection profile from the site survey (*Hakuho Maru* cruise 96-3-1), the lithostratigraphic column developed from coring at Site 1179, and depths predicted for lithostratigraphic boundaries. The lithostratigraphic column was scaled to the seismic section using the velocity-depth relationship of Carlson et al. (1986) to calculate the two-way traveltime of unit boundaries and ash layers derived from core observations. In the lithostratigraphic column, solid lines = unit boundaries; dotted lines = ash layers. Lithostratigraphic boundary depths are given in meters next to the column.



**Figure F14.** Close-up photograph of the typical clay- and radiolarian-bearing diatom ooze of Unit I (interval 191-1179B-4H-5, 88–120 cm).

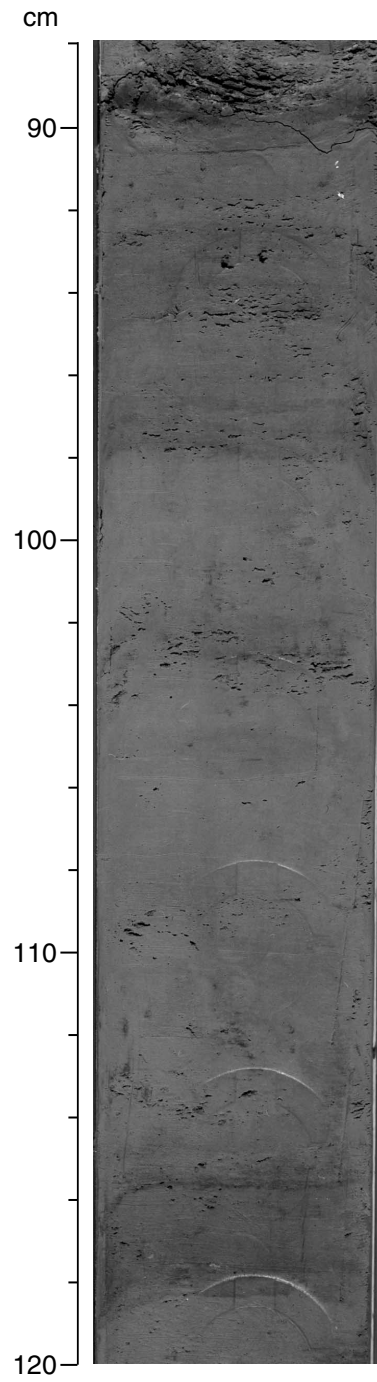


Figure F15. Close-up photograph of typical clay-rich diatom-bearing radiolarian ooze of Unit II (interval 191-1179C-20H-6, 30–50 cm).

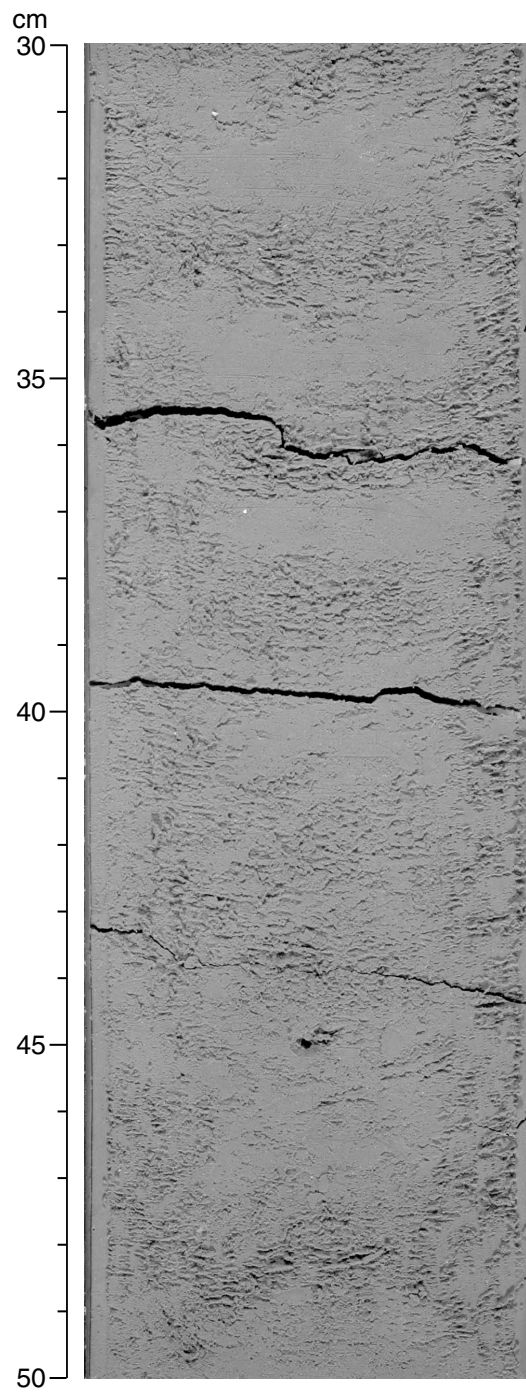


Figure F16. Close-up photograph of brown pelagic clay found in Unit III (interval 191-1179C-24H-5, 72–91 cm).

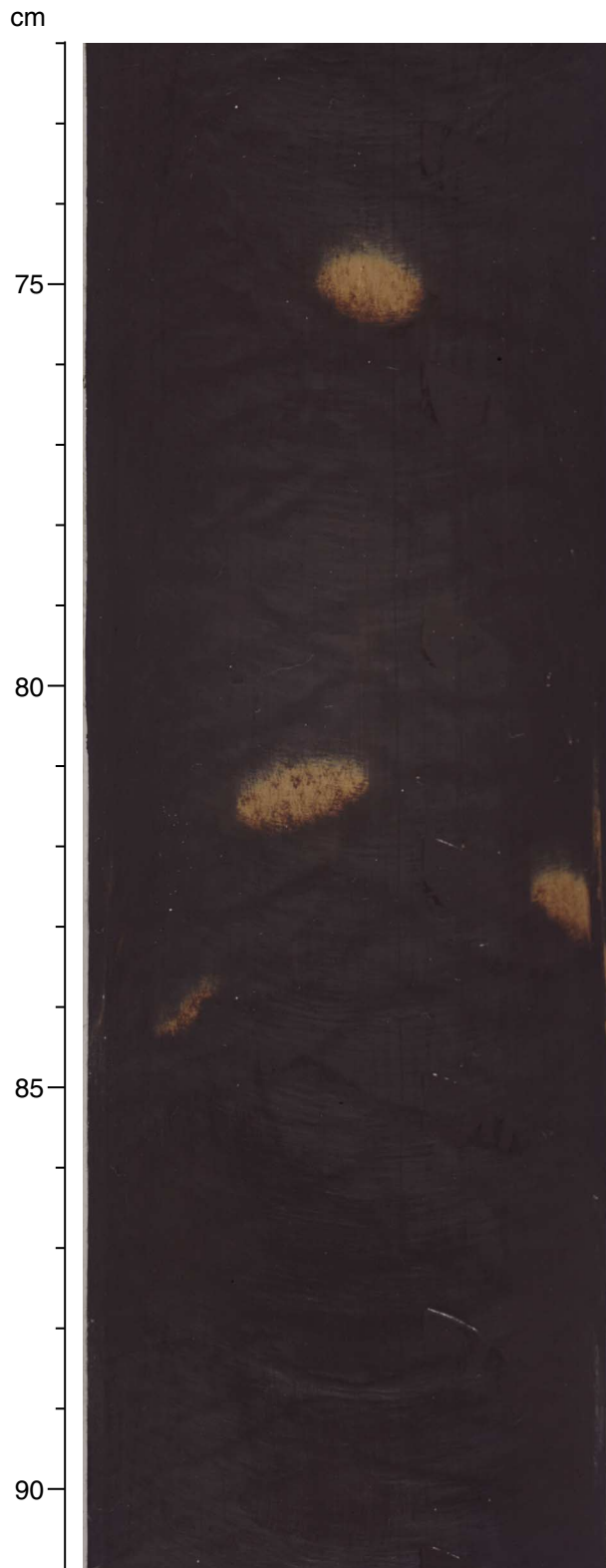


Figure F17. Close-up photograph of chert fragments recovered from Unit IV (interval 191-1179D-6R-1, 80–110 cm).



**Figure F18.** Close-up photograph of basalt from Unit V. Lighter areas are interpillow sediments (interval 191-1179D-11R-1, 74–102 cm).

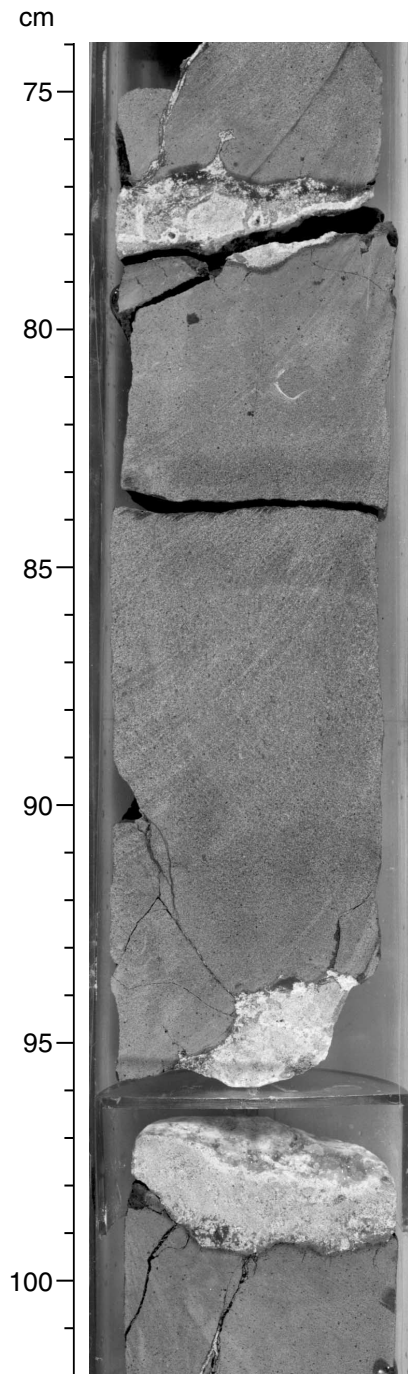
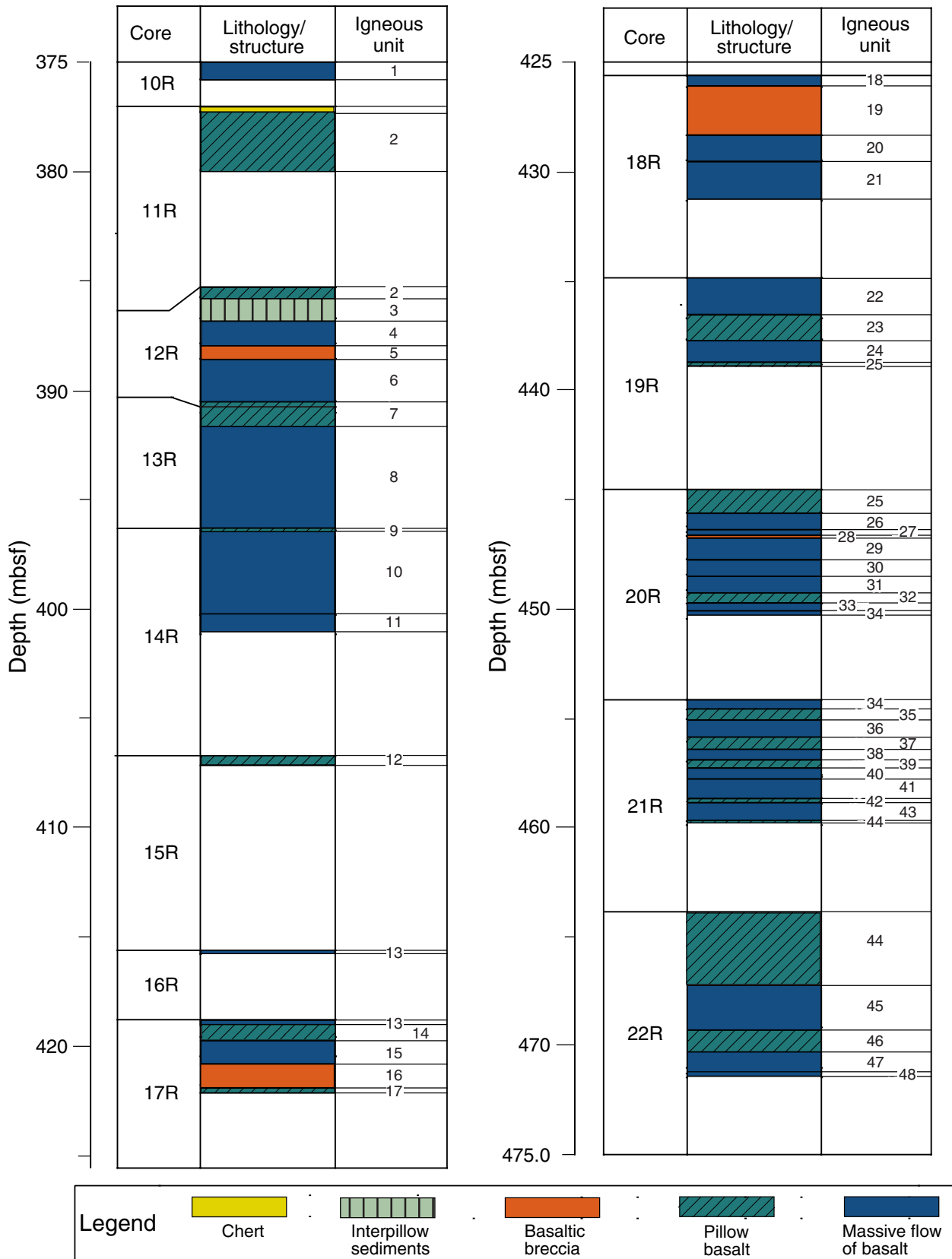


Figure F19. Summary of igneous units in the basaltic basement section (lithostratigraphic Unit V).



**Figure F20.** Age-depth curve for Site 1179 developed from biostratigraphic data. Dashed lines = radiolarian datums. Minimum and maximum ages for each sample constrain sediment accumulation rates and are shown as shaded areas; a best-fit sedimentation rate curve was fitted through the shaded region, with uncertainty represented by the darker gray wedge.

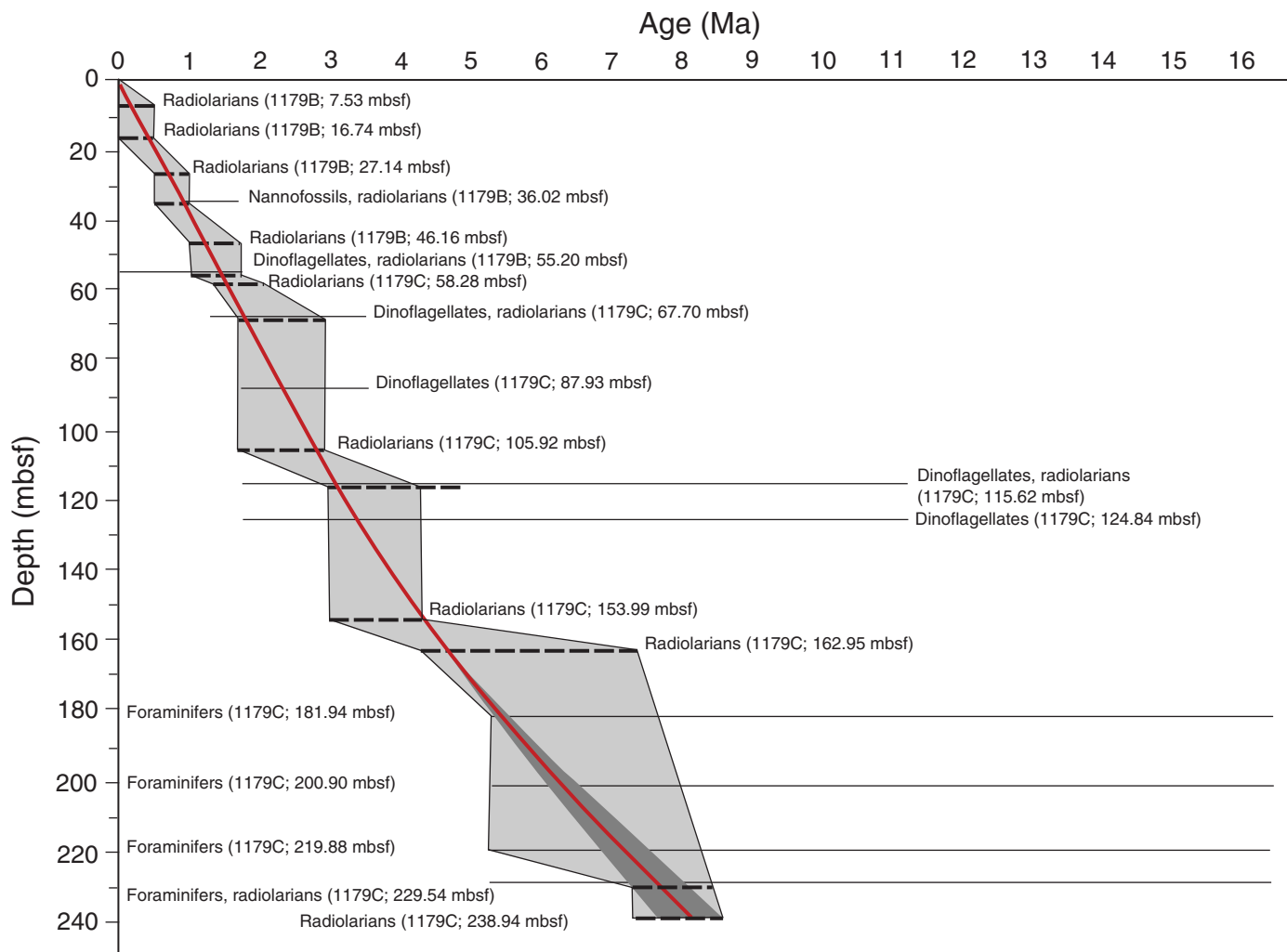
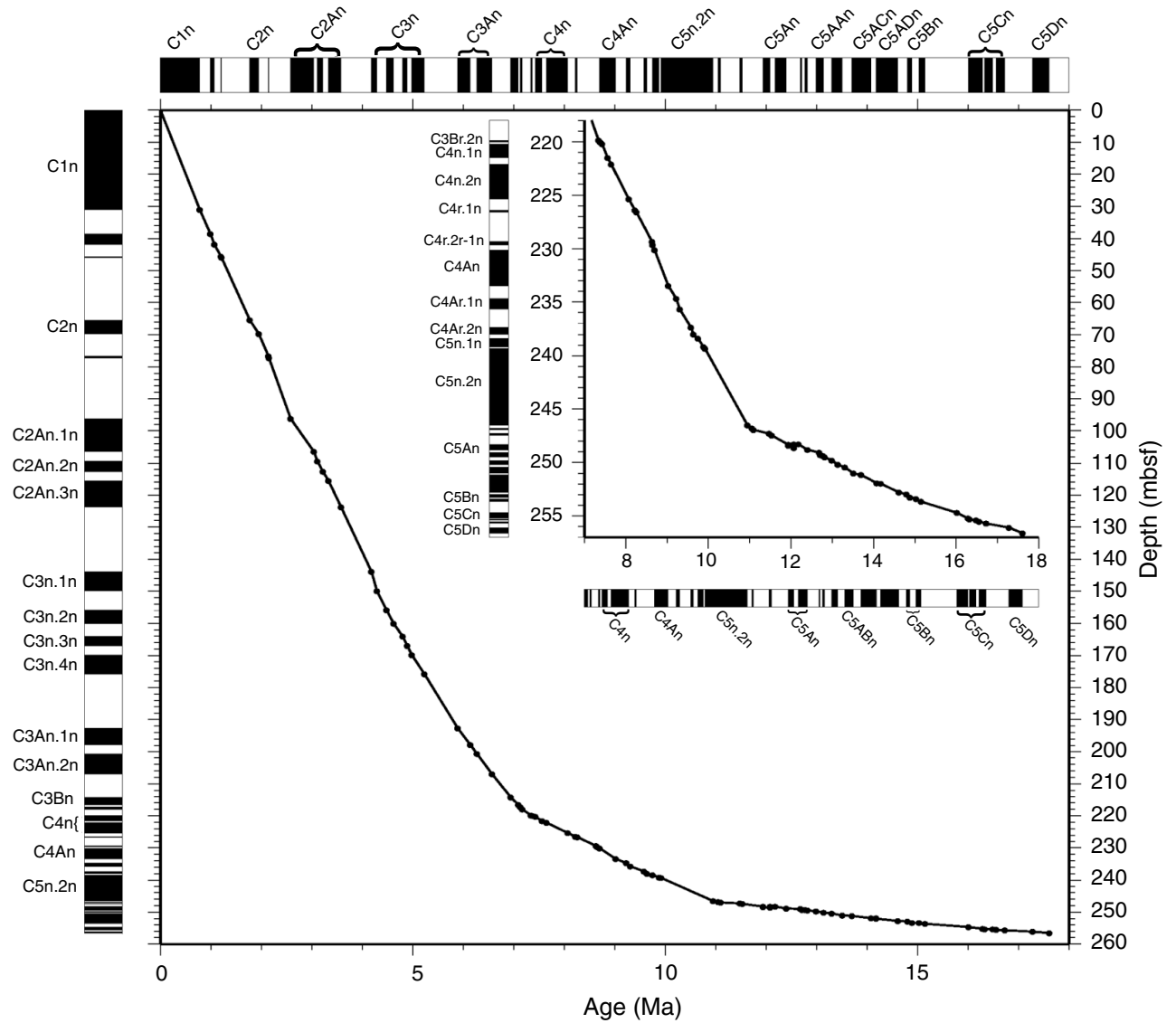


Figure F21. Age-depth curve for Site 1179 from magnetostratigraphic interpretations of paleomagnetic data. The magnetic polarity reversal time scale is from Berggren et al. (1995). Black bands = normal polarity; white bands = reversed polarity.



**Figure F22.** Summary figure showing velocity, density, and porosity vs. depth at Site 1179. The lithostratigraphic column is shown at the left. Solid circles in the bottom plots represent measurements taken in the basaltic basement. Plots at the top show measurements taken in the sedimentary section. Open triangles and circles show data from discrete measurements, whereas solid circles show MST-derived data. ([Figure shown on next page.](#))

Figure F22 (continued). (Caption shown on previous page.)

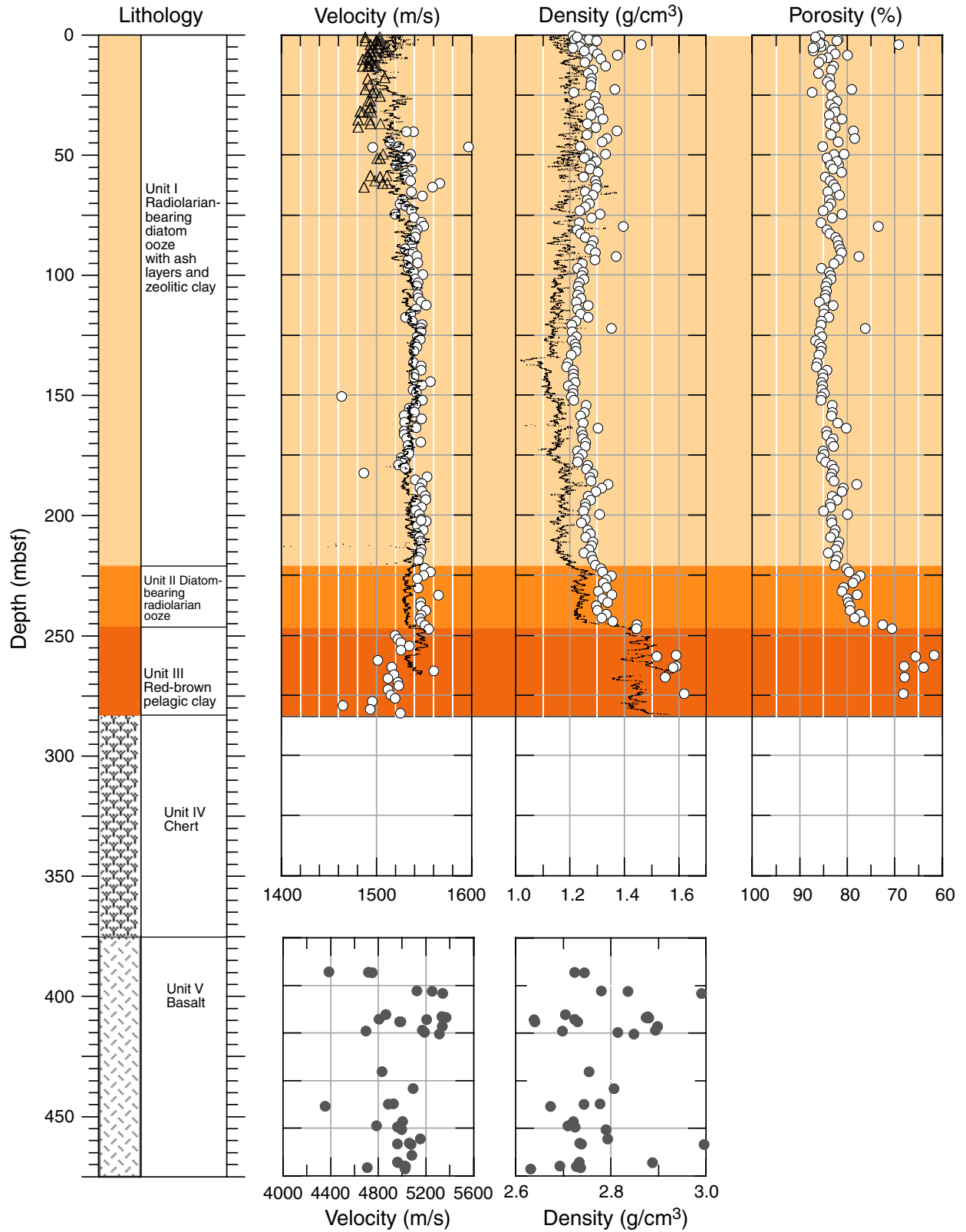


Table T1. Operations summary, Leg 191.

Hole	Latitude	Longitude	Water depth (m)	Number of cores	Interval cored (m)	Core recovered (m)	Recovery (%)	Interval drilled (m)	Total penetration (mbsf)	Time on hole (hr)
1179A	41°04.7884'N	159°57.7877'E	5565.5	1	10.0	10.1	100.7	0.0	10.0	18.00
1179B	41°04.7887'N	159°57.7879'E	5563.9	6	55.1	55.9	101.4	0.0	55.1	11.75
1179C	41°04.7871'N	159°57.7856'E	5563.9	27	249.9	246.9	98.8	43.0	292.9	70.50
1179D	41°04.8122'N	159°57.7862'E	5566.0	22	194.0	50.4	26.0	281.0	475.0	177.50
1179E	41°04.7729'N	159°57.7973'E	5565.9	0	0.0	0.0	0.0	475.0	475.0	362.75
Site 1179 totals:				56	509.0	363.2	65.3	719.0	1307.0	580.50
1180A	14°19.25'N	144°48.00'E	2145.5	0	0.0	0.0	0.0	0.0	5.0	18.00
1180B	14°19.25'N	144°48.00'E	2145.5	0	0.0	0.0	0.0	0.0	8.0	0.50
1180C	14°18.51'N	144°44.84'E	2120.5	0	0.0	0.0	0.0	0.0	3.0	1.75
Site 1180 totals:				0	0.0	0.0	0.0	0.0	16.0	20.25
1181A	14°19.25'N	144°48.00'E	983.5	0	0.0	0.0	0.0	0.0	3.0	2.25
1181B	14°19.25'N	144°48.00'E	969.4	0	0.0	0.0	0.0	0.0	3.0	2.00
1181C	14°19.25'N	144°48.00'E	958.4	0	0.0	0.0	0.0	0.0	3.0	6.75
Site 1181 totals:				0	0.0	0.0	0.0	0.0	9.0	11.00
1182A	12°57.0'N	143°36.6'E	2862.3	0	0.0	0.0	0.0	0.0	2.0	7.00
1182B	12°57.0'N	143°36.6'E	2866.3	0	0.0	0.0	0.0	0.0	1.5	0.50
1182C	12°57.0'N	143°36.6'E	2866.3	0	0.0	0.0	0.0	0.0	5.0	5.75
1182D	12°57.0'N	143°36.6'E	2865.3	0	0.0	0.0	0.0	0.0	3.0	10.75
1182E	12°57.0'N	143°36.6'E	2865.3	0	0.0	0.0	0.0	0.0	4.5	9.00
1182F	12°57.0'N	143°36.6'E	2860.3	0	0.0	0.0	0.0	0.0	3.8	3.75
1182G	12°57.0'N	143°36.6'E	2861.3	0	0.0	0.0	0.0	0.0	5.0	16.50
Site 1182 totals:				0	0.0	0.0	0.0	0.0	24.8	53.25

**Table T2.** Extended operational summary, Leg 191.

Hole	Number of APC cores	Number of XCB cores	Number of RCB cores	Seafloor (mbrf)	Rig floor elevation (m)	Total penetration (mbrf)	Comments
1179A	1	0	0	5576.5	11.0	5586.5	
1179B	6	0	0	5574.4	11.0	5629.5	
1179C	24	3	0	5576.7	12.8	5869.6	
1179D	0	0	22	5577.0	11.0	6052.0	
1179E	0	0	0	5577.0	11.1	6052.0	Hole dedicated to seismometer package installation
Totals:	31	3	22	5576.3	11.4	5822.7	
1180A	0	0	0	2157.0	11.5	2162.0	HRRS spud tests
1180B	0	0	0	2157.0	11.5	2165.0	HRRS spud tests
1180C	0	0	0	2132.0	11.5	2135.0	HRRS spud tests
Totals:	0	0	0	2148.7	11.5	2154.0	
1181A	0	0	0	995.0	11.0	998.0	HRRS spud tests
1181B	0	0	0	981.0	11.6	984.0	HRRS spud tests
1181C	0	0	0	970.0	11.6	973.0	HRRS spud tests
Totals:	0	0	0	982.0	11.4	985.0	
1182A	0	0	0	2878.0	11.7	2880.0	HRRS spud tests
1182B	0	0	0	2878.0	11.7	2879.5	HRRS spud tests
1182C	0	0	0	2877.0	11.7	2882.0	HRRS spud tests
1182D	0	0	0	2870.0	11.7	2873.0	HRRS spud tests
1182E	0	0	0	2872.0	11.7	2876.5	HRRS spud tests
1182F	0	0	0	2873.0	11.7	2876.8	HRRS spud tests
1182G	0	0	0	2873.0	11.7	2878.0	HRRS spud tests
Totals:	0	0	0	2874.4	11.7	2878.0	

Note: APC = advanced hydraulic piston corer, XCB = extended core barrel, RCB = rotary core barrel, HRRS = hard-rock reentry system.